Faculty of Aerospace Engineering

Ecological Interface Design: Sensor Failures in Air Traffic Control Decision-Making

V.A. Bijsterbosch

June 22, 2015

Ecological Interface Design: Sensor Failures in Air Traffic Control Decision-Making

Master of Science Thesis

For obtaining the degree of Master of Science in Aerospace Engineering
at Delft University of Technology

V.A. Bijsterbosch

June 21, 2015

Faculty of Aerospace Engineering · Delft University of Technology

Delft University of Technology

Delft University Of Technology
Department Of
Control and Operations

The undersigned hereby certify that they have read and recommend to the Faculty of Aerospace Engineering for acceptance a thesis entitled **"Ecological Interface Design: Sensor Failures in Air Traffic Control Decision-Making"** by **V.A. Bijsterbosch** in partial fulfillment of the requirements for the degree of **Master of Science**.

Dated: June 21, 2015

Readers:

prof.dr.ir. M. Mulder

dr.ir. M. M. Van Paassen

dr.ir. C. Borst

dr.ir. J. C. F. De Winter

Acronyms

ADS-B	Automatic Dependent Surveillance - Broadcast
AH	Abstraction Hierarchy
ATC	Air Traffic Control
ATCo	Air Traffic Controller
C&S	Control & Simulation
CD&R	Conflict Detection & Resolution
DURESS	DUal Reservoir Simulation
DUT	Delft University of Technology
EID	Ecological Interface Design
FBZ	Forbidden Beam Zone
GPS	Global Positioning System
INS	Inertial Navigation System
KBB	Knowledge-Based Behavior
PID	Piping-and-Instrumentation Diagram
PR	Primary Radar
PZ	Protected Zone
RBB	Rule-Based Behavior
SBB	Skill-Based Behavior
SRK	Skills, Rules & Knowledge
SSD	Solution Space Diagram
SSR	Secondary Surveillance Radar
SSSI	Single-Sensor Single-Indicator
SVD	Synthetic Vision Display
WDA	Work Domain Analysis

Contents

List of Figures

Part I

Final Master of Science Thesis Paper

Ecological Interface Design: Sensor Failures in Air Traffic Control Decision-Making

V. A. Bijsterbosch
MSc Student Control & Operations
Aerospace Engineering
Delft University of Technology

dr.ir. C. Borst & dr.ir. M.M. Van Paassen
Assistant & Associate Professors
Control & Simulation
Aerospace Engineering
Delft University of Technology

prof.dr.ir. M. Mulder
Professor Control & Simulation
Aerospace Engineering
Delft University of Technology

***Abstract*—Ecological Interface Design (EID) is an interface design framework widely used in process control work domains, and more recently also for aviation purposes. An example is the Solution Space Diagram (SSD), a decision-support tool for air traffic controllers designed according to the EID principles. However, there have been some concerns about the performance robustness of ecological interfaces when subjected to incorrect sensor information. This paper presents research that was performed to investigate the effects of explicitly visualizing the means-ends relationships on sensor failure detection performance. The set-up and findings of a human-in-the-loop experiment with sixteen subjects controlling aircraft in a predefined airspace show promising results. An analysis of the experimental data indicate that the ecological interface with explicit representation of the means-ends relations enables improved failure detection performance. Advisory response times turned out to be longer, indicating the usage of this extra functionality in order to check the advisories. Specifically in high complexity scenarios subjected to sensor failure, this extra feature has a positive impact on performance.**

I. Introduction

In order to deal with an increasing number of challenges in terms of safety, economical and environmental issues, future Air Traffic Management (ATM) systems will tend towards more automated systems, enabling air traffic controllers to deal with the predicted growth in air traffic movements [1]. It is expected that automation will become more advanced and will play an important role in decision-making support for controllers. However, in complex work domains like ATM, unexpected and unanticipated events cannot be eliminated and cannot be handled by fully automated systems only. Therefore, the creativity and adaptability of human experts will remain a crucial aspect in dealing with uncertain, stochastic systems such as in the aviation domain. It is for this reason that a design philosophy like Ecological Interface Design (EID) focuses on designing human-machine interfaces where automation serves as a team-player that supports decision-making of controllers, rather than replacing the human factor completely by automated systems. The starting point of EID is to analyze the work domain to better understand the structure and constraints wherein the system operates. The interaction between automation and human controllers, ideally, is facilitated by ecological interfaces that represents the boundaries and constraints of the work domain in a way that resonates with the mental model of the controller. The challenge lies in representing the required information such that it fully supports knowledge-based problem-solving and decision-making, which is exactly the type of behavior needed in case of unanticipated events, e.g., when sensors fail.

One of the main challenges of ecological interfaces is the susceptibility of such a system to sensor noise. There are some doubts about the robustness of performance when dealing with incorrect sensor information [2]. Studies in primarily process control domains have already shown that ecological interfaces have equal or even better sensor failure detection performance compared to conventional interfaces [3]–[5], and also in aviation applications promising results have been found [6]. However, missing in literature is research about the influence of explicitly representing the means-ends relations of the Abstraction Hierarchy (AH) on sensor failure detection performance. The EID framework reasons that only if all relevant information is presented and the relations between the various elements of abstraction are made visible to the end-user, a system can be controlled effectively. Any irregularities in expected system behavior can then be correlated through the work domain constraints and interface cues resulting in functional redundancy. It is therefore hypothesized that the explicit relations in terms of visual cues will have a positive contribution to sensor failure detection performance.

This research intends to fill that gap answering the following main research question: *Does an ecological interface that explicitly represents the means-ends relations of the abstraction hierarchy give the controller improved support for sensor failure detection?* Furthermore, the effects of sensor failure presence and increased scenario complexity on the performance and workload are investigated. A human-in-the-loop experiment in an Air Traffic Control (ATC) simulator has been designed, with sixteen participants using the Solution Space Diagram (SSD) [7], an ecological interface designed for Conflict Detection & Resolution (CD&R) in ATC. The means-ends relations are then manipulated to find out if this will positively contribute to the sensor failure detection performance of the controllers.

This paper is structured as follows. First, the interface design framework underlying this research is briefly described in Section II, giving a summarized background on the design methods and discussing potential pitfalls of EID. This design approach is used in the interface design of the SSD tool, which is presented in Section III, which also discusses a geometric analysis of the tool. This interface is used in a human-in-the-loop experiment to test the theoretical framework. Section

V discusses the set-up of the executed experiment, followed by the presentation of the experimental results in Section VI. Finally, Section VII ends the paper with conclusions and recommendations for future work.

II. Theoretical Motivation

Before discussing the SSD tool used for this research, the underlying theoretical framework known as EID will be shortly elaborated on, along with the concerns regarding sensor failure, which lies at the basis of this research.

A. Ecological Interface Design

The interface design framework EID was first introduced by Kim J. Vicente and Jens Rasmussen in order to increase safety in process control work domains [2]. This design philosophy focuses on making constrains and relationships in the complex cognitive work domain visible to the end-user, enabling the end-user to limit its core activities to higher order problem solving and decision making. In order to develop an efficient interface, a Work Domain Analysis (WDA) should be performed, revealing the physical and intentional constraints. In the aviation domain investigated here, and more specifically air traffic control, some of these constraints are the aircraft performance specifications (physical) and separation regulations (intentional). A decomposition tool known as the AH can be used to identify all different elements of the domain at different levels of abstraction, which are linked by means-ends relations [8]. The lowest levels represent the physical mechanisms and objects, including the sensors providing the raw data that is integrated in the interface. The importance of the AH is well stated by St-Cyr et al.: *"An interface that represents the system constraints at multiple levels of abstraction may continue to provide a correct account of the constraints at one level of abstraction when those at another level are violated."* [5] This is a crucial realization for this research, which studies the effect of visualizing means-ends relations on performance when subjected to sensor failure. The AH of the SSD will be presented in Section III-B, which is used to evaluate which means-ends relations should be made explicitly visible for the purpose of sensor failure detection.

A better understanding of the work domain and its elements of abstraction and constraints should specifically benefit the controller when dealing with unfamiliar and unanticipated events, at which point the human primarily relies on Knowledge-Based Behavior (KBB), opposed to Rule-Based Behavior (RBB) or Skill-Based Behavior (SBB) [2]. KBB requires a higher understanding of the underlying principles of the system, which is exactly what EID strives to represent in these interfaces through the AH. In the ATC domain for example, it is desired to visualize the velocity range of aircraft, while at the same time showing the constraints in terms of obstruction induced by other aircraft. If however, an unanticipated event may occur, e.g., a sensor failure causing false (surveillance) information to propagate through the system, the controller relies on KBB and an advanced level of reasoning to solve the problem. There are not always standard rules available for such situations, and the controller needs to use its creative and innovative mind combined with its mental model of the system to solve these events. Indicating means-ends relations between different levels of the AH can take some of the cognitive workload away, e.g., deriving *locomotion* and *obstruction* directly from sensor information in the case of ATC. This releases controllers from these efforts such that they can focus primarily on problem solving and decision-making. Especially in the ATC domain, which is characterized by aircraft flying at high velocities in relatively small airspace, little room is allowed for time-consuming integration of different sensors and decision-making.

B. Concerns Regarding Sensor Failure Detection

In order to control a complex system, sensors are used to collect and display information about the state of the work domain. Configuring and visualizing these individual variables in an organized and logical way will create emergent features, indicating task-relevant variables that can be used for higher-order problem solving and decision making. In the case of the ATC system, the controller requires information about aircraft locations, velocities, headings etc. to construct an image of the air traffic flow. This information can be obtained by surveillance systems (e.g. radar, Automatic Dependent Surveillance - Broadcast (ADS-B), etc.). Instead of focusing on integrating all these variables mentally, it is beneficiary to have this information presented in a way that instinctively indicates higher order elements like *locomotion* and *obstruction*. This ecological way of representing the control problem should reduce the cognitive workload of the operator, since the required variables are integrated and do not need to be derived from lower-level sensors. In order to implement the EID philosophy to an application, several obstacles have to be overcome. One of the main concerns identified in literature [2], [9]–[11], is the robustness of performance when the system is subjected to sensor failure.

One of the greatest concerns thus far is the effect that noisy or faulty sensors have on operator performance. The hypothesis on this specific topic is two-fold. On the one hand, one can reason that an EID interface is resilient to incorrect sensor information, due to explicit representation of the redundant constraints by the means-ends links of the AH. On the other hand, one can argue that system operators would easily confuse the displayed state of the work domain with the actual state, *because* the constraints are visualized and easy to perceive [9], [10]. In EID, these analytical tools can be used and implemented in the interface as a means such that the operator can make a well-informed decision on sensor fault diagnosis, meaning that the operator remains responsible. The idea is that if the higher-order functional constraints are explicitly visualized in the interface, it should be easier for the system operator to identify broken constraints, e.g., to diagnose a faulty sensor. It should be noted that this also depends on the interpretation of the operator. By making a proper WDA of the controlled system using and AH, the designer is able to identify the information necessary for operators to deal with the complete working spectrum of the system, including unanticipated events.

The main difference between the EID approach on sensor fault detection and the approach by classical control theorists is the influence of the human factor on the system. Several analytical models for fault detection have been developed, based on parity equations, parameter estimation and state estimation methods [12], [13]. By comparing an analytical reference model to the actual state of the system, an unexpected deviation of the residual can lead to a sensor fault detection and diagnosis. Control theorists, however, argue that fault diagnosis should be completely automated using these analytical models. The fear is that human factors will cause faulty sensors to be overlooked. However, such a model will only account well for familiar and anticipated events. When an unfamiliar and unanticipated event will occur, the analytical reference model might be inadequate to detect and diagnose sensor failure. Therefore, in EID, it is believed that the human capacity, in the sense of adaptability, creativity and flexibility, plays a crucial role in decision-making in control problems. These cognitive capabilities activated during KBB are crucial in the complex work domain of human-machine systems. If the whole system is automated, humans would not possess a clear mental model of the controlled system and are unable to intervene in these situations.

C. Previous Research

Several studies already indicate a comparable or improved performance in sensor failure detection when comparing conventional interfaces with ecological interfaces. Research done by Reising and Sanderson, involving a micro world process pasteurization control system called the Pasteurizer II, report an experiment investigating the differences of an EID interface over the conventional Piping-and-Instrumentation Diagram (PID) for minimal and maximal adequate instrumentation set-up. It showed that the maximally adequate EID interface showed the best failure diagnosis performance over the conventional PID. The main conclusion drawn in this research is that interfaces should display all relevant information to the operator, which becomes crucial in unanticipated events like sensor failures [4]. Similar comparison studies between conventional and ecological interfaces in process control [3], [5] and aviation [6] show similar promising results.

In an investigation focused more profoundly on the means-ends relations, Ham et al. compared three ecological displays of a cooling control system of a pressurized water reactor nuclear power plant on fault detection performance [14]. Out of three displays, the display explicitly visualizing means-ends relations between the generalized and abstract function levels showed significant increased operator performance, indicating an improved awareness of the system, enabling the controller to solve unexpected situations. The role of explicit means-ends relations has not yet been tested on aviation applications, therefore this research uses the SSD interface for CD&R purposes in ATC.

The primary difference between process control and aviation domains is the time window in which they operate. Process control systems are relatively slow and static, while in aviation decision-making often takes minutes, if not seconds, to avoid conflicts or accidents, and these open systems are highly dynamic. It is therefore very interesting to investigate how this time pressure factor will influence the performance in an ATC experiment using the SSD, and what the contribution of the means-ends relations can be.

III. The Solution Space Diagram

This research focuses on finding the effect of explicitly visualizing the means-ends relations of the AH on sensor failure detection and diagnosis. The interface used for the experiment is the SSD, of which will be discussed in this section.

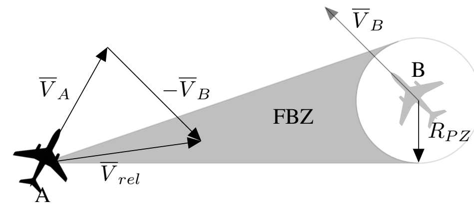

(a) Untranslated conflict zone.

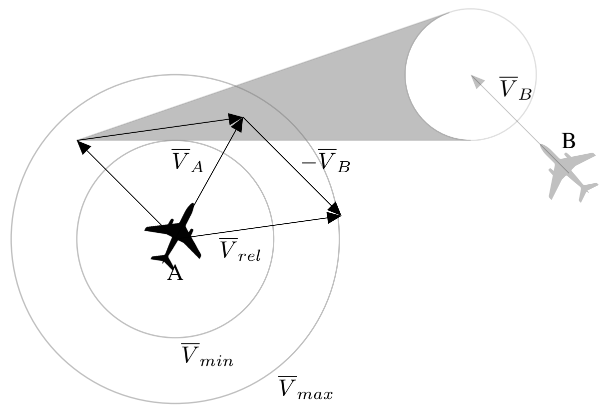

(b) Translated conflict zone.

Fig. 1. Construction of the SSD.

A. Main Working Principles

A novel ecological interface proposed to contribute to the solution of the growing air traffic is called the SSD. The original SSD developed by Van Dam et al. was designed to enable airborne self separation in terms of speed and heading of aircraft in the proximity of conflict situations [7]. Later on this was further developed to investigate its use for ATC purposes [15], [16]. The main goal of this version is to ensure the separation criteria, defined by a disk with height of 2,000 ft. and 5NM radius called the Protected Zone (PZ). The SSD is an ecological constraint-based interface, which uses the states of aircraft (internal performance constraints) and separation criteria in terms of a PZ (external separation constraints), indicating the solution space in terms of heading and speed. This enables controllers to resolve conflicts and avoid Loss of Separation (LoS) by giving instructions to aircraft.

Figure 1a displays two aircraft, aircraft A with velocity vector $\overline{V}_A$ and aircraft B with velocity vector $\overline{V}_B$. Their relative velocity vector $\overline{V}_r$ is displayed at the origin of aircraft A, indicating how aircraft A moves with respect to aircraft B. Any combination of $\overline{V}_A$ and $\overline{V}_B$ such that $\overline{V}_r$ is located in the grey colored triangle called the Forbidden Beam Zone (FBZ), leads to a LoS. This visualization is inconvenient because controllers use absolute instead of relative velocities.

In order to solve this, the FBZ is translated by the velocity

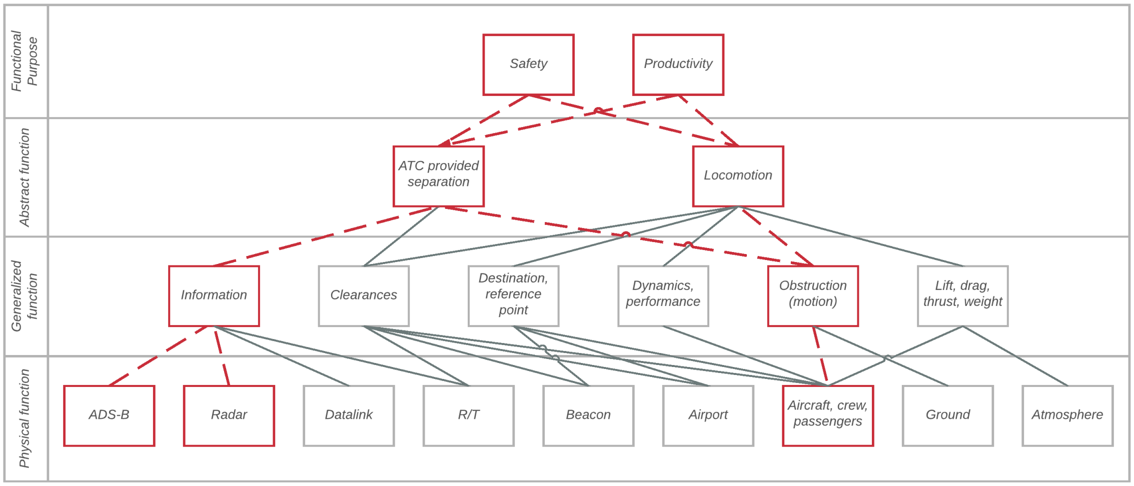

Fig. 2. Abstraction Hierarchy of the SSD including the means-ends relationships.

vector $\overline{V}_B$ of aircraft B, as shown in Figure 1b. It shows the same situation as in Figure 1a, however due to the translation a conflict only occurs if $\overline{V}_A$, and not $\overline{V}_r$, lies in the FBZ. The purpose is to make it more intuitive for the air traffic controller to recognize where the solution space lies, enabling the controller to redirect aircraft A outside the FBZ and resolving the conflict. The external constraints are therefore defined by the FBZ. The internal constraints in terms of minimum and maximum velocity are indicated by two circles, wherein the controller can give clearances.

B. Means-Ends Relationships

According to Vicente, performance can be improved by integrating structural means-ends relationships spatially and temporally [10]. The added functionality in the SSD will be discussed here using the abstraction hierarchy shown in Figure 2.

Referring to the AH of the SSD in Figure 2, one can see that several elements at different abstraction levels are connected to each other by the so-called means-ends relations, as explained in Section II-A. The rectangle element representing *Aircraft* at the physical function level of the AH is related to *Obstruction (motion)* element at the generalized function level, which in its turn is related to the *ATC provided separation* and *Locomotion* elements at the abstract function level. In order to create more transparency for the controller about which aircraft is causing which FBZ (*Obstruction*) on the SSD, it can be beneficiary to make the means-ends relations more explicitly visible in the interface, i.e., by highlighting the FBZ and corresponding aircraft with visual cues.

Located in the bottom left side of the physical function level are the *Radar* and *ADS-B* system, which are means to *information ends* for the construction of the SSD. Using both these surveillance systems creates redundancy. The radar is used to construct the overall traffic image, whilst the ADS-B is used to construct the FBZ and SSD. As mentioned before, the FBZ links *Locomotion* with *Obstruction* and *Aircraft* elements. However, if the system state information provided from the radar or ADS-B to ATC is incorrect, a mismatch occurs between actual system state and provided system state information. This may result in incorrect *ATC provided separation*. Taking into account the redundancy of the combined surveillance systems, it is expected that explicitly visualizing the relations will help sensor failure detection.

The explicit means-ends representation will create two important emergent features. First, by hovering with the mouse over the observed aircraft it is possible to identify which observed aircraft causes which part of the obstruction for the controlled aircraft, and which does not. The FBZ of the observed aircraft is highlighted in the SSD of the controlled aircraft. This is a bottom-up reasoning in the AH, since the physical function element *Aircraft* is linked explicitly to the generalized function element *Obstruction* by hovering over the aircraft icon.

Second, it is possible by right-clicking on the conflict area of the SSD (the cumulative FBZ's of all observed aircraft) to identify which aircraft create obstruction to that specific point on the SSD. This is a top-down reasoning in the AH, since the abstract function element *Locomotion* is linked explicitly to the generalized function element *Obstruction* and the physical function element *Aircraft* by right-clicking on the FBZ.

This should help the controller identify the aircraft on the SSD and linking the FBZ with radar image, especially in complex traffic situations. More importantly, it is expected to help the controller detect and identify aircraft transmitting incorrect ADS-B position information.

IV. Sensor Failure Propagation

An ADS-B accuracy study is performed in combination with a geometric analysis of the SSD in order to find out how typical ADS-B failures will propagate through the interface.

A. ADS-B Accuracy

The hypothetical interface used in this experiment simulates the use of data from radar to construct the overall traffic situation and ADS-B to construct SSD. In order to introduce realistic ADS-B sensor failures, a literature study has been performed to investigate the type and magnitude of frequently occurring errors. Below is a list of studies that have been looked into:

1) London TMA [17]
2) Several Southern European air navigation service providers [18]
3) Ground stations spread around Europe [19]
4) Route Chengdu to Jiuzhai, China [20]
5) Beijing FIR region, China [21]

These studies show alarming results with respect to ADS-B latencies and horizontal position accuracy, with frequently occurring position errors reaching up to measured errors of 7.5NM in magnitude. One of the main causes for ADS-B not meeting the performance standards is frequency congestion, caused by other avionics using the same 1,090MHz frequency spectrum. [22]. The type of ADS-B error introduced in the experiment is a horizontal position error of 7.5NM in order to keep it realistic, but as well as visible to the naked eye on the SSD interface. In order to prevent confounds and to keep the experiment measurable and simple, speed or heading errors are omitted for this research.

B. Geometric Analysis

In principle, several state properties of the observed aircraft can be derived from the FBZ drawn in the SSD of the controlled aircraft, which can be used to mentally reconstruct the conflict geometry purely by looking at the SSD.

1) The relative bearing of the observed aircraft can be derived by looking at the location of the tip of the bisector of the FBZ.
2) The velocity vector of the observed aircraft is indicated by the location of the tip of the bisector of the FBZ, indicating magnitude and heading.
3) The FBZ width angle indicates the distance towards the observed aircraft; a wider FBZ corresponds to a closer observed aircraft.
4) The rate at which the FBZ width angle changes indicates the closure rate of the aircraft.

To determine which order of magnitude a change in location has on the FBZ and SSD, a geometric analysis of the SSD and FBZ has been performed.

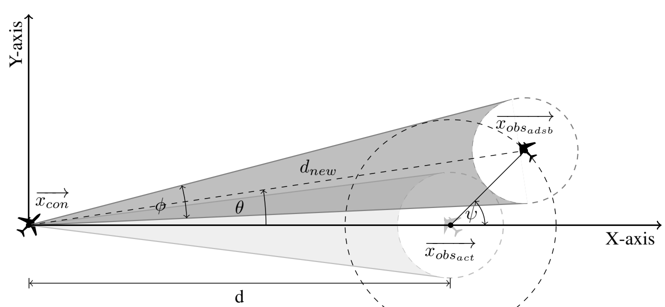

Fig. 3. Sensitivity analysis geometry.

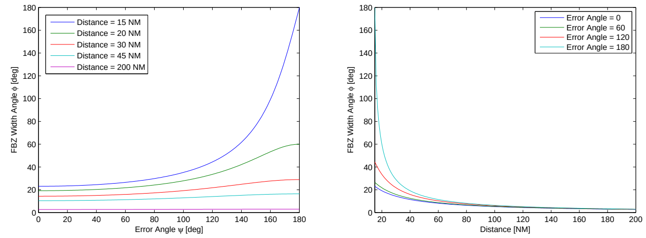

(a) (b)

Fig. 4. Forbidden Beam Zone width angles for various distances and error angles.

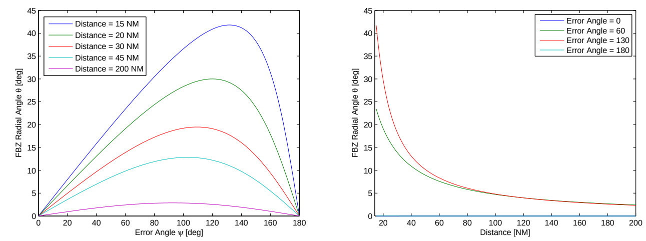

(a) (b)

Fig. 5. Forbidden Beam Zone radial angles for various distances and error angles.

Figure 3 shows the locations of three aircraft, namely the location of the controlled aircraft $\overline{x}_{con}$, the actual location of the observed aircraft indicated by radar $\overline{x}_{obs_{act}}$, and the location of the observed aircraft given by incorrect ADS-B data $\overline{x}_{obs_{ADSB}}$. Furthermore, the width angle of the FBZ created by $\overline{x}_{obs_{adsb}}$ is indicated with ϕ, while the ADS-B error angle is indicated with ψ. The angle of the difference in orientation between $\overline{x}_{obs_{act}}$ and $\overline{x}_{obs_{ADSB}}$ is given by θ, and the distance between actual location of the observed aircraft and the controlled aircraft is indicated by d. Simple geometric calculations lead to the changing width and radial angles as functions of distance and error angle, as shown in Figures 4 and 5.

Figure 4a shows a general effect on FBZ width angles for error angles over $100\,\text{deg}$, and Figure 5a shows a noticeable effect between $40\,\text{deg}$ and $160\,\text{deg}$ on FBZ radial angles. Therefore, for the final experiment conflict geometries the error angle should range between $100\,\text{deg}$ and $160\,\text{deg}$. Figures 4b and 5b conclude that up to approximately 50NM distance the FBZ width and radial angles change significantly. The further away aircraft are, the less influence error angles have on FBZ width angles. On a radar screen image showing a large airspace these changes are difficult to distinguish, so therefore the measurements are taken for conflicting aircraft at a distance of 50NM and closer. This analysis, together with a preliminary experiment, proved that in-track position off-sets at far distances are more difficult to distinguish than off-track errors at close distance. The results of this analysis are used in designing the scenarios, conflict geometries and determining the timing of advisories for the experiment, as will be discussed in Section V-E. The sensor failures are implemented in the simulator for the experiment, and it is expected that the explicit visualization of the linkes of the AH

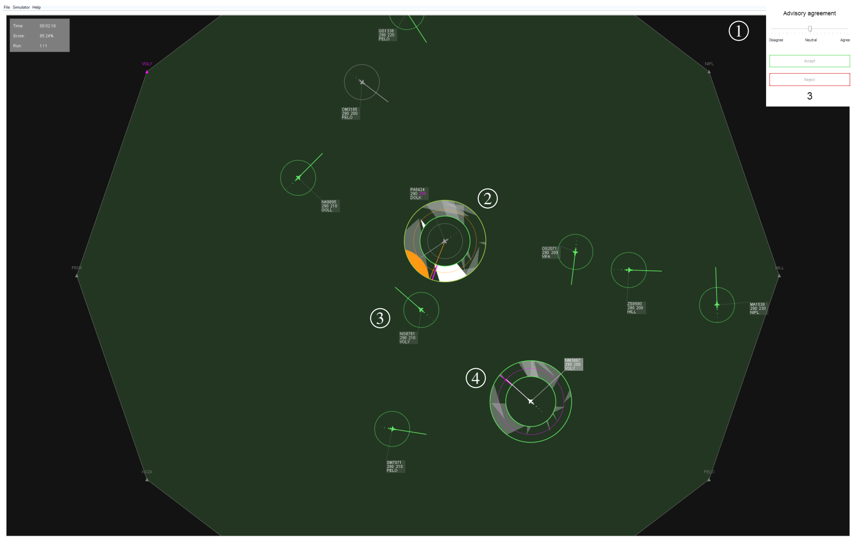

Fig. 6. Screenshot of the ATC simulator at the moment of an advisory.

in combination with the sensor redundancy help the controller detect these failures.

V. Experiment Design

An experiment has been designed and conducted to investigate whether or not explicitly representing the means-ends relations of the AH positively contributes to sensor failure detection and diagnosis, as is hypothesized in EID theory. The SSD interface is used as a CD&R tool for ATC, which is simulated in the Multidimensional Framework for Advanced SESAR Automation (MUFASA) environment, of which a screenshot can be found in Figure 6.

A. Apparatus

The MUFASA simulator is a Java-based application enabling air traffic controllers to command aircraft in a given airspace, using the SSD tool. Figure 6 shows a screenshot of the simulator during an advisory, showing the agreement rating window on the top right (①) and two open SSD's, one for the advisory (②) and one manually opened by the controller (④). Aircraft ② is in conflict with aircraft ④. Furthermore, a FBZ is highlighted due to the mouse hovering over the manually opened aircraft.

The air traffic motion is simulated by simple, linear kinematic equations. These are described by the aircraft position coordinates, velocity and heading angle. In order to simulate aircraft turn dynamics and the transient in changing magnitude of aircraft velocity, first order transfer functions are used [16].

B. Independent Variables

In order to answer the research questions, three independent variables were defined, resulting in a mixed within- and between-subjects experiment.

First, the between-subjects variable is the explicit representation of the means-ends relations, resulting in two different interfaces tested by two separate groups. This will from now on be referred to as **group I** (means-ends relations off) and **group II** (means-ends relations on).

Second, a within-subjects variable is the scenario complexity, resulting in two levels, namely low (**L**) and high (**H**). The scenario complexity is a derivative of structured versus unstructured air traffic flow. By keeping the aircraft number in the sector approximately the same at all time, the average conflict-free solution space for the unstructured, high complexity situation is smaller, as can be seen in Figure 7.

Third, a within-subjects variable is the sensor failure, which can be either off (**N**) or on (**Y**). The sensor failure is always an ADS-B position off-set of 7.5NM, which was found to be a realistic, frequently occurring error. In the scenarios with a sensor failure, only one aircraft emits incorrect ADS-B position data to the system.

C. Control Variables

The SSD version used for this research is the Time-To-Contact (TTC), meaning that the time it takes for a LoS to occur is color-coded in darkgrey (over 180 sec.), orange (between 90 and 180 sec.) and red (between 0 and 90 sec.), as can be seen in Figure 6. These visual cues should help the controller prioritize which conflicts are critical and need urgent attention. In order to avoid confounds, all aircraft used in the scenarios are of the same class, meaning they have the same performance envelope (velocity range) at that altitude. Scenarios with mixed aircraft classes can result in a FBZ lying outside the SSD. Furthermore, the airspace sector dimensions are kept the same for all scenarios, with a decagon shape of 50NM radius.

Two means to control aircraft are available. First, if a conflict occurs, the automation will give a resolution advisory and the controller has 30 seconds to accept or reject that score, after which the advisory expires and is automatically executed (management-by-exception [23]). Second, when the advisory is accepted, rejected or expired, that specific aircraft is enabled for manual control. This can all be done by a regular mouse and keyboard input.

The main reason for supervisory control through management-by-exception instead of complete manual control is to keep the experiment controllable in order to test certain traffic situations. Research shows that a higher level of decision-making automation authority results in lower automation acceptance [24], [25]. This is the main reason to keep the automation at a fairly low-level. The advisories are scripted, however the participants are told that the advisories are generated by automated checking of conflicts and exit points deviations. The advisories are based on the information from the SSD, which on its turn is generated by ADS-B data. Since this research is focused on the operator performance with an interface subjected to ADS-B sensor failure, the operator will be confronted with cases where the SSD is inconsistent with the overall traffic situation visualized by the radar. This means that there are test cases wherein an advisory is given that is actually correct according to the SSD, but which is in fact incorrect and misleading, possibly resulting in a new conflict. These specific cases are of interest to investigate the sensor failure detection and diagnosis. The advisories are designed in such a way that they are as efficient as possible, within the boundaries of the aforementioned restrictions.

In order to test multiple traffic situations per scenario, and to keep the scenarios repeatable and interesting, the simulation ran at 3-times faster than real time. This resulted in a traffic scenario of 585 seconds, which ran for 195 seconds in the simulation. This was chosen as such that four consecutive advisories of 30 seconds could be given, with 15 seconds of initial adjustment time, 15 seconds in between advisories, and 15 seconds of manual run-out time after the last advisory. A 1Hz update frequency was used in order to simulate an actual radar revolution rate.

D. Dependent Measures and Resolution Advisories

Several measurements were taken of which the most interesting are listed here;

- **Correct accept/reject score** measures if a participant agrees with the advisory or wants to implement an own solution.
- **Advisory agreement rating** measures the level of agreement with the given advisory, which was measured by a slider bar with scale 0-100 before responding to the advisory.
- **Sensor failure detection** is measured using verbal comments and is noted if the correct sensor failure was detected and corresponding aircraft identified.
- **Workload rating** measures the overall perceived workload measured using a slider bar with scale 0-100 at the end of each scenario
- **Advisory response time** measures the time between initiation of, and a possible response to an advisory.
- **Number of inspections** is recorded in order to see how often a SSD would be opened, and furthermore how many means-ends inspections are utilized.
- **Number of LoS** are measured as a means of performance.

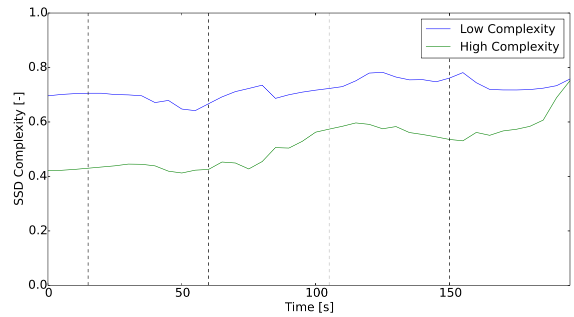

Fig. 7. Average available solution space complexities over time.

In addition to these primary measures, a few other measures were logged to further support the analysis. These were: minimum separation distance between aircraft, collisions and manual velocity and heading commands.

E. Traffic Scenarios

Following the independent variables, experimental conditions can be determined, namely **A:LxN** (Scenario **A**, **L**ow complexity, **N**o sensor failure), **B:LxY**, **C:HxN** and **D:HxY** for groups I and II, resulting in a total of eight conditions. The scenario complexities are measured according to the SSD metric, showing the instantaneous average solution space of aircraft within the sector, whereas a higher number means a higher available solution space. These are plotted over time in Figure 7, giving an average complexity of 0.7188 for low complexity scenarios (more solution space) and 0.5146 for high complexity scenarios (less solution space). There are two reasons the complexities converge towards the end of the scenario. First, because towards the end of the scenario there are no more aircraft flying into the sector, the number of head on traffic situations are reduced, increasing the solution space (specifically for the high complexity case). Second, due to manual input of the controller, sub-optimal solutions were found, increasing the solution space (extra margins) at the expense of efficiency. The aircraft count was approximately the same over the two scenarios.

Two repetitions of each condition were performed. In order to prevent recognition, dummy scenarios were used between actual measurement scenarios and measurement scenarios were rotated 180 degrees. In order to prevent confounds, only one type of conflict geometry was used for the actual measurement points, namely a converging tracks situation. A preliminary conducted experiment and SSD geometry analysis showed that this type of conflict geometry was best suited to test performance when subjected to sensor failure, compared to overtaking tracks. Also, these investigations showed that sensor failures at large distances were practically impossible to notice with the bare eye, restricting the advisories to relatively developed conflict situations with less than a minute to LoS.

The resolution advisories aim at solving conflicts in an efficient matter, whilst trying to steer the aircraft towards their designated exit points, as much as possible. Figure 8a indicates a typical conflict, where the advisory (red arrow) suggests the conflicting aircraft to go behind the other two aircraft. It may deviate from the exit point (magenta line) because the first

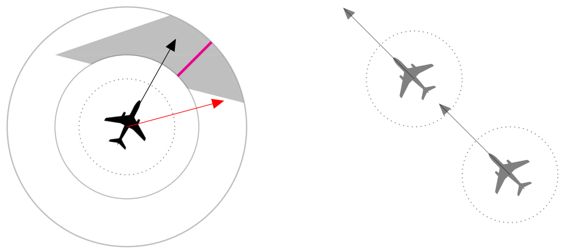

(a) Conflict geometry and advisory without sensor failure.

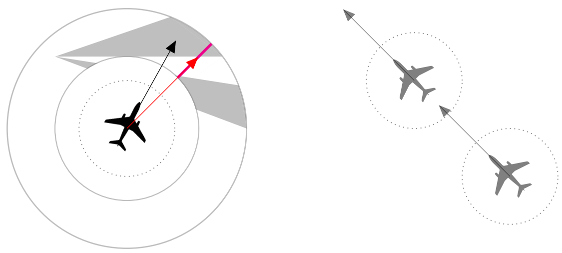

(b) Conflict geometry and advisory with sensor failure.

Fig. 8. Typical conflict geometries in the experiment.

priority is to solve the conflict, and second priority is to direct aircraft as much as possible towards exit point. It is then the responsibility of the controller to manually redirect the aircraft to its exit point, once the two aircraft in line have passed.

In case of sensor failure, the advisories are based on the partially incorrect SSD. The advisory is restricted to a location in the heading/velocity-spectrum where the SSD indicates it to be correct, while in reality the resolution is incorrect and would direct that aircraft into a conflict with the aircraft sending erroneous position information. This can be seen in Figure 8b, showing exactly the same situation as Figure 8a, only this time the bottom right aircraft gives incorrect position information. The SSD visualizes this aircraft to be 7.5NM behind its actual current location, indicating solution space between the two aircraft that is actually not present. This should be the case for the full 30 seconds the advisory is given, which seriously restricts the options for advisories in the case of failure. Due to these limitations, it was not always possible to follow the rules of the air [26], and often an optimal resolution is used in terms of time efficiency or path length. It is then measured whether or not the subjects accept or reject that incorrect advisory, indicating a distrust towards the automation based on the SSD, and hence detecting the sensor failure. In the scenarios including a sensor failure, three of the four advisories would be affected by this failure and would thus be incorrect.

F. Subjects and Control Task

Sixteen persons participated in the experiment, all students or researchers in the faculty of Aerospace Engineering at the TU Delft. Their experience varied from working in ATC and ATM domains to aircraft control systems.

The control task given to the subjects was two-fold, namely:

1) **Conflict resolution task** The primary control task is to ensure safe separation at all times between aircraft by resolving potential conflicts.
2) **Exit clearance task** The secondary control task is to ensure all aircraft exit the sector airspace at their designated exit points, as much as possible.

As mentioned before, both control tasks can be completed by accepting or rejecting a given automated resolution advisory within 30 seconds, and additionally by executing manual commands to those aircraft. It is emphasized to the participants to always carefully check the advisories based on the SSD with the overall traffic situation given by the radar image.

G. Hypotheses

The following hypotheses are formulated with respect to the expected results.

- **H1: Enabling the explicit representation of the means-ends relations (group II) in the SSD will increase operator performance of sensor fault detection.** Enabling the explicit means-ends representation will create two important emergent features as discussed earlier in Section III-B. These features explicitly show higher-order properties of the AH of the system, here the locomotion and obstruction of the observed aircraft. This integrated representation will save the operator quite some cognitive workload on deriving the necessary information from the sensors. In terms of operator performance on sensor fault detection, it is expected that due to that lower required cognitive workload, a sensor failure will be easier detected, and the type of the error can be diagnosed more accurately. It is expected that this also reflects in the comparison between the correctly rejected scores of the groups, meaning it is presumed that group II has more correctly rejected advisories.
- **H2: Increasing the air traffic scenario complexity will decrease the operator performance of sensor fault detection using SSD relatively more for group I compared to group II.** It is hypothesized that a higher scenario complexity leads to a higher workload experienced by the controller [27], and thus resulting in a lower performance. Several studies have already shown specifically for the SSD that with increasing air traffic scenario complexity, the overall operator workload is increasing and its overall performance is declining [15], [16], [28], [29]. It is expected that this trend will also take place in this experiment, both with and without explicit representation of means-ends relations. A higher sector complexity leads to more overlapping FBZ, making it difficult for the operator to distinguish which FBZ belongs to which aircraft. Therefore, it is expected that with disabled means-ends relations the performance is relatively more decreasing with increasing scenario complexity, compared to enabled explicit means-ends relations.
- **H3: Both higher scenario complexity and inducing a sensor failure in a scenario will lead to an increased perceived workload.** It is expected that an unstructured, high complexity scenario increases

stress levels, which will reflect on the workload scores [27]. Furthermore, if a scenario is subjected to a sensor failure, it is hypothesized that controllers notice that the corresponding SSD and resolution advisory are not compliant with the radar image. This can increase the experienced stress level and workload.

- **H4: Sensor failure presence will result in lower agreement ratings, specifically for group II.** Since some advisories are directly affected by sensor failures, it is expected that the agreement ratings will be lower for these scenarios. Referring to hypothesis H1 it is anticipated that this effect is more noticeable for group II.

VI. Results

Following the verbal comments during the experiment and the debriefing, there was no indication of scenario or conflict situation recognition of the repeated measures by any of the subjects. The data of the experiment was logged and analyzed. First, it was checked which data fulfilled the normality requirements in order to perform Analysis of Variance (ANOVA) statistical tests. This was done using Kolmogorov-Smirnov and Shapiro-Wilk normality tests. It turned out that the agreement ratings, workload ratings, advisory response time and number of inspections can be considered normally distributed. All other data were subjected to non-parametric tests in order to look for statistical significance, where a Kruskal-Wallis test was used to search for between-subject effects, and a Friedman test was used to investigate within-subjects effects.

A. Correct Accept/Reject Score

The correct accept and reject scores are an indication of the advisory agreement of the subjects. An initial analysis was performed by plotting the cumulative accept and reject scores, as shown in Figure 9 and Figure 10.

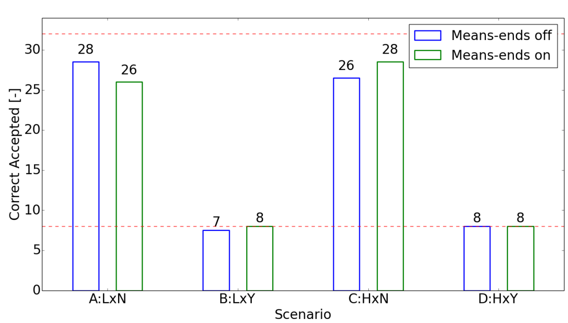

Fig. 9. Cumulative number of correct accept advisories.

The maximum correct accept score for scenarios without sensor failure (**N**) is 32 (four correct advisories times eight participants per group), and for scenarios with sensor failure (**Y**) is four (one correct advisory times eight participants per group), which are indicated by red dotted lines. At first sight, a distinct trend can be spotted between the presence of sensor failure and the number of correct accepted advisories. There does not seem to be a significant difference for the accept scores between groups, which is confirmed by a Kruskal-Wallis test. A Friedman test shows there are within-subjects interactions ($\chi^2(1) = 43.596, p < 0.001$), which are caused by sensor failure presence. No effects of complexity can be found on the number of correct accept score.

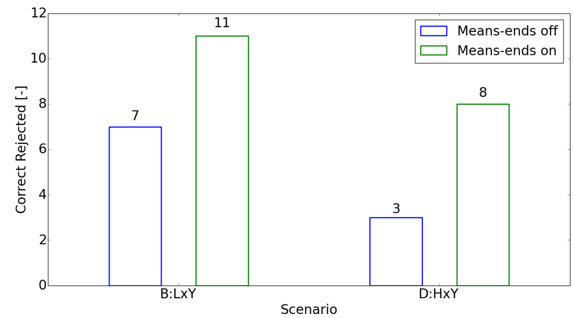

Fig. 10. Cumulative number of correct rejected advisories.

For the reject scores, there seems to be a trend between groups, whereas the means-ends relations seems to contribute to a higher number of correct rejected advisories. Also, a trend can be seen between low and high complexity scenarios, whereas a lower complexity leads to a higher number of correct rejects. The maximum correct reject score is 24 (three incorrect advisories times eight participants per group). It can therefore be deduced from the results that quite often incorrect advisories were accepted, which can be related to the different control strategies discussed in Section VI-G. A Kruskal Wallis test showed there is no significant difference between the two group distributions for scenarios B ($\chi^2(1) = 1.049, p = 0.306$) and D ($\chi^2(2) = 4.000, p = 0.406$). A Friedman test showed within-subject interaction effects ($\chi^2(1) = 4.445, p = 0.035$), as confirmed by a post-hoc Wilcoxon test ($Z = -2.365, p = 0.018$), indicating that there is a negative correlation of scenario complexity with correct rejected advisories, as was expected.

B. Agreement Rating

Agreement ratings are given for every advisory to indicate the level of compliance with the given resolution. These scores were normalized and analyzed using boxplots, shown in Figure 11. An overall trend can be seen between the presence or absence of a sensor failure, whereas the failure presence leads to a lower agreement rating. Furthermore, this effect seems to be larger if the explicit means-ends relations are enabled, resulting in more extreme ratings for this group.

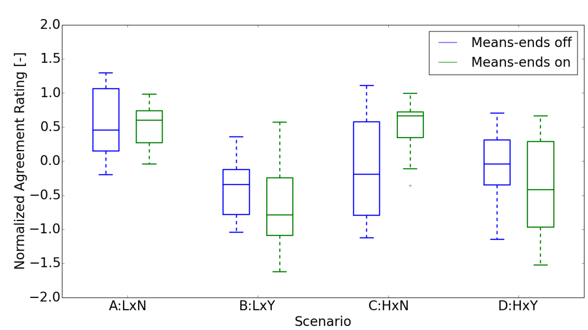

Fig. 11. Normalized agreement rating.

Using a 2x2x2 three-way mixed ANOVA test a significant main effect of sensor failure presence ($F(1, 14) = 19.283, p = 0.001$) is found on agreement rating. However, no significant main effects of group and complexity are found, nor any interaction effects.

C. Sensor Failure Detection

Sensor failure detection is measured through verbal comments. Only when the participants found the correct aircraft subjected to sensor failure, this would be recorded. The cumulative numbers of detection are shown in Figure 12, whereas a maximum cumulative result of eight was possible (one failure per scenario times eight participants), indicated by a red dotted line. It can be seen that the explicit means-ends relations result in an overall higher detection number for both scenarios. A trend can also be detected for complexity, whereas a lower complexity leads to a higher number of detected failures.

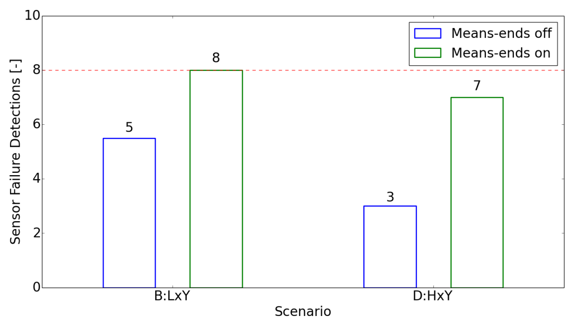

Fig. 12. Sensor failure detection.

After performing a Kruskal-Wallis test it is shown that both conditions show a significant difference between the two groups, namely for scenario B:LxY $\chi^2(2) = 4.923, p = 0.027$ and for scenario D:HxY $\chi^2(2) = 5.208, p = 0.022$. It can be seen that this difference is relatively bigger for the high complexity case. A Friedman test also indicates a significant difference within subjects, where a higher complexity would give a lower sensor failure detection rate $\chi^2(1) = 4.500, p = 0.034$.

D. Workload Rating

After each scenario subjects completed a workload score varying from 0-100. These scores were then normalized and plotted as can be seen in Figure 13. No clear distinction between groups can be directly found, however in the presence of sensor failure participants tend to rate a higher workload compared to scenarios without failure. A 2x2x2 three-way mixed ANOVA test showed no overall main effects between groups. A main effect of sensor failure presence is found ($F(1, 14) = 56.573, p < 0.001$), where a failure presence leads to higher workload rating. No effect of group, complexity or interaction effects are found.

E. Response Time

The advisory response time was defined as the time between the start of the advisory and accepting, rejecting or expiring. The results are plotted in Figure 14. It can be

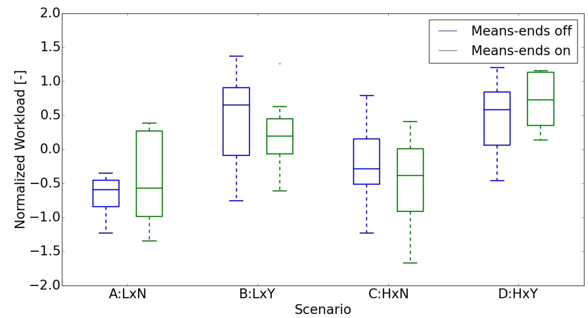

Fig. 13. Normalized workload rating.

observed that if the means-ends relations are enabled, the trend seems to be that advisory response time is consistently longer. Also, the presence of a failure seems to lead to overall longer response times, as well as a higher complexity does. A 2x2x2 three-way mixed ANOVA test was performed, showing a hint of different distributions ($F(1, 14) = 206.249, p = 0.051$), indicating an effect of the means-ends relations on the time., however this is not significantly sufficient from a statistic point of view. A significant main effect of complexity ($F(1, 14) = 14.328, p = 0.002$) and sensor failure presence ($F(1, 14) = 10.233, p = 0.006$) is found, meaning that a both a higher complexity and/or the presence of a failure leads to longer response times. No interaction effects were found between group, complexity and sensor failure presence.

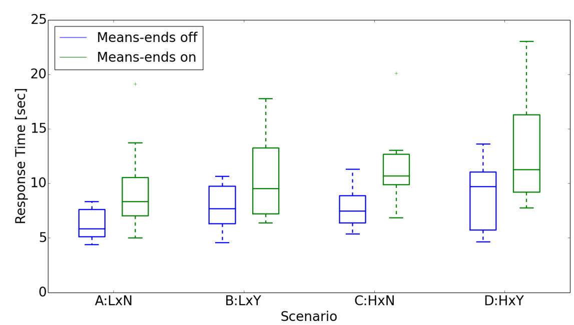

Fig. 14. Advisory response time.

F. Inspections

To find out more about the interface usage, the total number of SSD inspections are counted and the boxplots are displayed in Figure 15. Even though the total values consistently show a higher number of inspections if the links are enabled, the variation within these groups is too high and no statistical significance in distributions is found ($F(1, 14) = 335.348, p = 0.144$). Main within-subjects effects are found for complexity ($F(1, 14) = 5.178, p = 0.039$), and failure ($F(1, 14) = 96.285, p = 0.050$). This indicates that both a higher complexity and a sensor failure presence lead to significant more SSD inspections.

For group II the usage of the extra functionality of means-ends relations is recorded. The right-mouse clicks are plotted in Figure 16, indicating no trends. Further investigation shows that some participants used this feature frequently, however

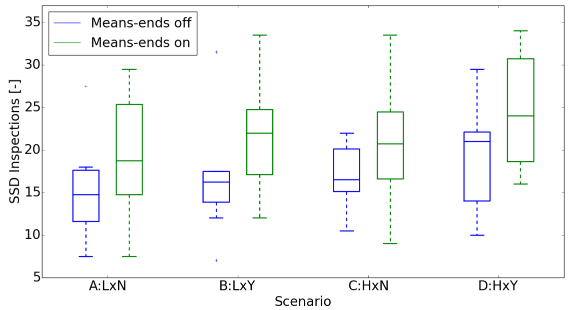

Fig. 15. Number of SSD inspections.

there were also three of the eight participants of group II that did not use this feature in any of the measured scenarios. No main effects of complexity and failure presence are found.

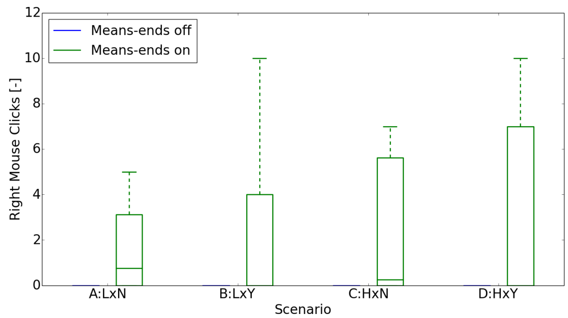

Fig. 16. Total means-ends inspections by right mouse click.

The usage of visualizing these relations by means of hovering over observed aircraft is shown in boxplots in Figure 17, which indicates no trends. No main effects are found for complexity and failure presence.

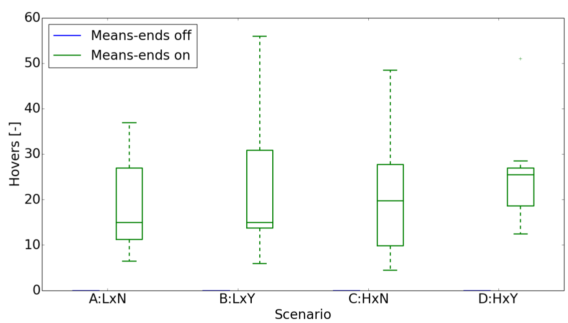

Fig. 17. Total means-ends inspections by hovering.

G. Control Strategies

Several control strategies could be identified from the data and observations, of which the most frequently occurring are briefly addressed in this section.

1) Check advisory with SSD, link FBZ to aircraft (mostly group II), and crosscheck this with radar image
2) Reject correct advisories and manually redirect (sometimes temporarily into FBZ) for larger margin
3) Accept/reject advisories such that aircraft is manually controllable, then implement manual resolution
4) Reject correct advisory, followed by manual resolution which is approximately the same as advisory

It can be seen that there were quite some different strategies used, which influenced the results. Some participants had more experience with ATC and have knowledge about the rules of the air, which influenced their judgment on the advisories. In some cases these participants would prefer mutual resolutions, however only one aircraft per conflict was enabled for manual control after the advisory. It must be noted that these participants were balanced over the two groups. Most participants also indicated to favor manual heading clearances over speed commands, as is confirmed by the results. The manual commands led in some cases to self-induced conflicts, resulting in a higher experienced workload. Due to these different control strategies, it is not always possible to correlate a rejected advisory with the logic used. The advisory could be rejected because a sensor failure was detected, or because the advisory was non-conform the desired resolution of the subject, or due to general reluctance to use automation. However, observations and verbal comments helped identifying which subjects correctly detected the aircraft subjected to sensor failure.

VII. Discussion

The goal of this research was to investigate the influence of explicit visualization of the means-ends relationships of the AH on the performance of the controller when the ATC system is subjected to ADS-B sensor failures. Participants had to control air traffic through a free route airspace, using the SSD ecological interface decision-support tool. Some scenarios were subjected to sensor failures, and it was investigated how that would affect operator performance, and if these failures could be detected. Furthermore, scenario complexity was manipulated by means of structuring the traffic in order to control the average solution space and workload per scenario.

A. Sensor Failure Detection Performance

Looking at the results, there are signs that explicit presentation of the means-ends relations of the AH enables improved support for controller performance when subjected to sensor failures. It is statistically proven that group II performed better at sensor failure detection than group I, therefore hypothesis H1 can be accepted. Verbal comments indicate that both groups could recognize that something was incorrect during sensor failure, however only group II was better able to identify the aircraft with failure. The extra information provided by explicitly visualizing the relations seems to help controllers to correctly identify problems, and manually come up with correct solutions. This is also partially supported by advisory response times and SSD inspections, where it appeared that group II uses more time and inspections to carefully check the SSD and the given advisory for correctness, however the difference is not statistically significant.

Furthermore, it is shown that this effect stronger is in unstructured, more complex situations. This is also partially supported by the correct reject scores, showing a trend between the groups, even though there is no confirmed statistical significant difference in distributions. As was hypothesized (H2), a higher complexity (unstructured scenario) leads to more overlapping FBZ's, which causes more trouble for group I. Even though the perceived workload was not necessarily higher for high complexity scenarios, the solution space was significant lower due to the unstructured nature of the free airspace, resulting in overlapping FBZ. Specifically in these type of situations, the means-ends relationships are useful for detecting sensor failures, therefore hypothesis H2 can be accepted. Due to the visualization of higher-order properties of the AH, an instinctive link can be made between locomotion and obstruction of aircraft. In combination with sensor redundancy this enables the controller to match the FBZ with the corresponding aircraft causing the obstruction. Using this information, the controller can then check if the advisory, that is based on the SSD, is safe in accordance with the overall radar image.

B. Automation Acceptance, Conformance and Strategies

The correct accept/reject scores showed no significant differences between group I and II. The high rate of (incorrect) advisory rejections can be explained by a number of reasons. First, there might be a lack of strategic conformance with the automation. Conformal resolution advisories are generally more easily accepted by the participant, i.e., if there is a mismatch between optimal resolution strategy of human and machine, the subject tends towards rejecting this advisory [30]. This conformance is personal and subjective, and might not always be the most optimal solution. The resolutions given in this experiment were in some cases due to sensor failure induced geometric restrictions not according to the rules of the air and thus not conformal with some subjects, even though in most cases the automated advisory was more optimal than the manual solution. Ideally, first a strategic conformance study should be performed along participants before the actual experiment, such that the preferred manual resolutions can be used to construct advisories, filtering out any conformance confounds [30].

Another reason for the number of (incorrect) advisory rejections could be that due to induced sensor failures, participants would get a dispositional automation bias. Due to a distrust towards the automation, which in some scenarios was based on an SSD subjected to erroneous sensors, some participants turned quite hesitant to accept advisories based on that automation, even in scenarios without incorrect information. This happened specifically with participants that had sensor failures in the first scenarios, indicating some order effects. This is in compliance with the work of Lee et al., indicating that there is a complex dynamic relation between trust and the use of automated advisories [31]. The variation in results can partly be appointed to different experiences within ATC and the knowledge of the rules-of-the-air, or lack thereof, and different developed strategies. Some participants based their strategies on visual support from the SSD only, while others tried to couple this information with the overall traffic scenario and relate this to the given resolution. For future research it is highly recommended to use a more homogeneous group of subjects for the experiment, ideally all with exactly the same background and knowledge. A longer training period could be beneficial for improved understanding of the system and development of consistent strategies.

C. Utilization of Means-Ends Relations

It can be seen that specifically the means-ends hovers were frequently used by all subjects of group II, while the right mouse click option was used by five of the eight subjects, and less frequently. One of the participants explained this behavior as follows: if an SSD of a random aircraft is open for inspection, it is possible that an advisory pops up opening a second SSD indicating the resolution for that aircraft, while the first SSD remains opened. However, the right-clicking function is still assigned to that first aircraft. Only first by left mouse clicking on the advisory aircraft would that enable the right mouse clicking. The reason for that is that if participants are inspecting an SSD and perhaps are preparing a manual command, it is undesired to interfere with this decision-making by prioritizing the advisory. This was also clearly indicated in the briefing and training, however the extra effort of clicking again can still be a reason for lower number of right-mouse click actions compared to hovers. Despite this, it can be said in general that the extra functionality is used quite extensively and helps the controller in task-relevant decision-making.

It can be stated that the visualization of the means-ends relations have a positive contribution in understanding the actual system state, and more precisely in correctly noticing any malfunction in information supply, specially in the presence of sensor redundancy. In the time-critical and highly dynamic aviation domain, these relations can help controllers with fast interpretation of information and decision-making. It should be noted, however, that due to this time pressure, some participants were not able to find a correct alternative solution. In none of the cases did the visual cues interfere with the controller activities or misinform the participant in any undesired way. It seems for those reasons that explicit visualization of means-ends relations can become increasingly important in sensor failure detection and diagnosis in ecological interfaces.

VIII. Conclusion

This paper presents the investigation of the effects of visualizing the means-ends relations of the Abstraction Hierarchy (AH) in an ecological interface on sensor failure detection performance. This is done by a conducting a human-in-the-loop experiment using a novel Air Traffic Control (ATC) ecological interface for Conflict Detection & Resolution (CD&R) called the Solution Space Diagram (SSD). It is hypothesized that an explicit visualization of these links helps the controller detect and identify sensor failures, improving performance. Sixteen subjects divided into two groups participated in the experiment, testing four conditions. It is shown that the added functionality of means-ends relations positively contributes to sensor failure detection. In some cases there were incorrect rejected advisories due to a lack of advisory conformance with the participants, or general reluctance to accept automation. However, the means-ends relations are extensively used in order to inspect the SSD and their advisories, resulting in a longer advisory response time and more accurate sensor failure detection performance. Visualizing the relations can therefore be a promising contribution to sensor failure detection performance for the SSD specifically and future ecological interfaces in general.

REFERENCES

[1] Eurocontrol, "Challenges of Growth 2013 Task 4: European Air Traffic in 2035," Tech. Rep., 2013.

[2] K. J. Vicente and J. Rasmussen, "Ecological Interface Design: Theoretical Foundations," *IEEE Transactions on Systems, Man and Cybernetics*, vol. 22, no. 4, 1992. [Online]. Available: http://ieeexplore.ieee.org/xpls/abs_all.jsp?arnumber=156574

[3] K. Christoffersen, C. N. Hunter, and K. J. Vicente, "A Longitudinal Study of the Effects of Ecological Interface Design on Deep Knowledge," *International Journal of Human-Computer Studies*, pp. 729–762, 1998. [Online]. Available: http://www.sciencedirect.com/science/article/pii/S1071581998901902

[4] D. V. C. Reising and P. M. Sanderson, "Minimal Instrumentation May Compromise Failure Diagnosis with an Ecological Interface." *Human Factors: The Journal of the Human Factors and Ergonomics Society*, vol. 46, no. 2, pp. 316–33, Jan. 2004. [Online]. Available: http://www.ncbi.nlm.nih.gov/pubmed/15359680

[5] O. St-Cyr, G. A. Jamieson, and K. J. Vicente, "Ecological Interface Design and Sensor Noise," *International Journal of Human-Computer Studies*, vol. 71, no. 11, pp. 1056–1068, Nov. 2013. [Online]. Available: http://linkinghub.elsevier.com/retrieve/pii/S1071581913001031

[6] C. Borst, M. Mulder, and M. M. Van Paassen, "Design and Simulator Evaluation of an Ecological Synthetic Vision Display," *Journal of Guidance, Control, and Dynamics*, vol. 33, no. 5, pp. 1577–1591, Sep. 2010. [Online]. Available: http://arc.aiaa.org/doi/abs/10.2514/1.47832

[7] S. B. J. Van Dam, M. Mulder, and M. M. Van Paassen, "Ecological Interface Design of a Tactical Airborne Separation Assistance Tool," *IEEE Transactions on Systems, Man and Cybernetics*, vol. 38, no. 6, pp. 1221–1233, 2008.

[8] K. J. Vicente, *Cognitive Work Analysis; Toward Safe, Productive, and Healthy Computer-Based Work*. Mahwah, New Jersey: Lawrence Erlbaum Associates, 1999.

[9] K. J. Vicente, N. Moray, J. D. Lee, J. Rasmussen, B. G. Jones, R. Brock, and T. Djemil, "Evaluation of a Rankine Cycle Display for Nuclear Power Plant Monitoring and Diagnosis," *Human Factors: The Journal of the Human Factors and Ergonomics Society*, vol. 38, no. 3, pp. 506–521, Sep. 1996. [Online]. Available: http://openurl.ingenta.com/content/xref?genre=article&issn=0018-7208&volume=38&issue=3&spage=506

[10] K. J. Vicente, "Ecological Interface Design: Progress and Challenges." *Human Factors: The Journal of the Human Factors and Ergonomics Society*, vol. 44, no. 1, pp. 62–78, Jan. 2002. [Online]. Available: http://www.ncbi.nlm.nih.gov/pubmed/12118874

[11] C. Borst, J. M. Flach, and J. Ellerbroek, "Beyond Ecological Interface Design : Lessons From Concerns and Misconceptions," *IEEE Transactions on Human-Machine Systems*, vol. 45, no. 2, pp. 164–175, 2015.

[12] R. Isermann, "Supervision, Fault-Detection and Fault-Diagnosis Nethodsan Introduction," *Control engineering practice*, vol. 5, no. 5, pp. 639–652, 1997. [Online]. Available: http://www.sciencedirect.com/science/article/pii/S0967066197000464

[13] P. M. Frank, "Fault Diagnosis in Dynamic Systems Using Analytical and Knowledge-Based Redundancy: A Survey and Some New Results," *Automatica*, vol. 26, no. 3, pp. 459–474, 1990. [Online]. Available: http://www.sciencedirect.com/science/article/pii/000510989090018D

[14] D. H. Ham and W. C. Yoon, "Design of Information Content and Layout for Process Control Based on GoalMeans Domain Analysis," *Cognition, Technology & Work*, pp. 205–223, 2001. [Online]. Available: http://link.springer.com/article/10.1007/s10111-001-8003-z

[15] G. A. M. Velasco, "Analysis of Air Traffic Controller Workload Reduction Based on the Solution Space for the Merging Task," *AIAA Guidance, Naviagtion and Control Conference*, no. August, 2010. [Online]. Available: http://arc.aiaa.org/doi/pdf/10.2514/6.2010-7541

[16] C. Borst, C. Westin, and B. Hilburn, "An Investigation into the Use of Novel Conflict Detection and Resolution Automation in Air Traffic Management," *SESAR Innovation Days*, no. November, 2012.

[17] B. Ali, A. Majumdar, W. Y. Ochieng, and W. Schuster, "ADS-B: The Case for London Terminal Manoeuvring Area (LTMA)," in *Tenth USA/Europe Air Traffic Management Research and Development Seminar*, 2013, p. 10.

[18] V. Cedrini, M. Zacchei, V. Zampognaro, E. Ente, N. Assistenza, V. Spa, and V. Agri, "ADS-B 1090ES Implementation : the CRISTAL-MED Project," vol. 3, pp. 1–5, 2010.

[19] C. Rekkas and M. Rees, "Towards ADS-B Implementation in Europe," *Tyrrhenian International Workshop on Digital Communications - Enhanced Surveillance of Aircraft and Vehicles*, pp. 1–4, 2008. [Online]. Available: http://ieeexplore.ieee.org/lpdocs/epic03/wrapper.htm?arnumber=4649019

[20] J. Zhang, W. Liu, and Y. Zhu, "Study of ADS-B Data Evaluation," *Chinese Journal of Aeronatics*, vol. 24(4), pp. 461–466, 2011.

[21] ICAO, "The Ninth Meeting of the Southeast Asia and Bay of Bengal Sub-regional ADS-B Implementation Working Group (SEA/BOB ADS-B WG/9)," Beijing, Tech. Rep., 2013.

[22] Y. Torel, "Is ADS-B Capable of Replacing Radar as a Primary Means of Aircraft Surveillance in the Near Future?" Delft University of Technology, Tech. Rep., 2014.

[23] R. Parasuraman, T. B. Sheridan, and C. D. Wickens, "A Model for Types and Levels of Human Interaction with Automation." *IEEE transactions on systems, man, and cybernetics. Part A, Systems and humans : a publication of the IEEE Systems, Man, and Cybernetics Society*, vol. 30, no. 3, pp. 286–97, May 2000. [Online]. Available: http://www.ncbi.nlm.nih.gov/pubmed/11760769

[24] D. B. Kaber and M. R. Endsley, *The Effects of Level of Automation and Adaptive Automation on Human Performance, Situation Awareness and Workload in a Dynamic Control Task*, Mar. 2004, vol. 5, no. 2. [Online]. Available: http://www.tandfonline.com/doi/abs/10.1080/1463922021000054335

[25] R. Parasuraman and V. Riley, "Humans and Automation: Use, Misuse, Disuse, Abuse," *Human Factors: The Journal of the Human Factors and Ergonomics Society*, 1997. [Online]. Available: http://hfs.sagepub.com/content/39/2/230.short

[26] ICAO, "Annex 2 to the Convention on International Civil Aviation: Rules of the Air," ICAO, Tech. Rep. July, 2005. [Online]. Available: http://link.springer.com/chapter/10.1007/978-3-642-25835-0_3

[27] I. V. Laudeman, S. G. Shelden, R. Branstrom, and C. L. Brasil, "Dynamic Density: An Air Traffic Management Metric," no. April, 1998. [Online]. Available: http://www.ntrs.nasa.gov/archive/nasa/casi.ntrs.nasa.gov

[28] R. Goritzlehner, C. Borst, J. Ellerbroek, C. Westin, M. M. Van Paassen, and M. Mulder, "Effects of transparency on the acceptance of automated resolution advisories," *IEEE International Conference on Systems, Man, and Cybernetics*, pp. 2965–2970, 2014. [Online]. Available: http://ieeexplore.ieee.org/xpls/abs_all.jsp?arnumber=6974381

[29] B. Beernink, C. Borst, J. Ellerbroek, M. M. Van Paassen, and M. Mulder, "Towards an Integrated Ecological Plan View Display for Air Traffic Controllers," Delft University of Technology, Tech. Rep., 2014.

[30] C. Westin, B. Hilburn, and C. Borst, "The Effect of Strategic Conformance on Acceptance of Automated Advice: Concluding the MUFASA Project," *Proceedings of the SESAR Innovation Days*, vol. 3, no. November, 2013. [Online]. Available: http://www.sesarinnovationdays.eu/files/SIDs/2013/SID-2013-18.pdf

[31] J. Lee and N. Moray, "Trust, Control Strategies and Allocation of Function in Human-Machine Systems," *Ergonomics*, 1992. [Online]. Available: http://www.tandfonline.com/doi/abs/10.1080/00140139208967392

Part II

Final Thesis Book of Appendices

Appendix A

Literature Study

This chapter summarizes the main points of the literature survey performed during the preliminary graduation phase, which are of interest for the rest of the graduation project on sensor failure in the Solution Space Diagram (SSD) ecological interface. According to Oxfords Dictionary, a (computing) *interface* can be defined as follows:

`interface` [ɪntəfeɪs] - *"a device or program enabling a user to communicate with a computer"*

as in for example *a graphical user interface* (Oxford University, 2014). It can be deducted from this definition that the function of an interface is to let the user of a computer system interact with this system. The interface should display all relevant information to the user, who on its turn can give input to that system. This chapter will elaborate more on all relevant literature on ecological interfaces like the SSD tool.

This chapter is structured as follows. First, the interface design framework used for the design of the SSD known as Ecological Interface Design (EID) is described in section A-1. The basic principles of the SSD ecological interface are described in section A-2. One of the main concerns in EID is its performance when facing sensor failures. This is elaborated on in section A-3, followed by a brief summary of an Automatic Dependent Surveillance - Broadcast (ADS-B) performance study in section A-4. The main conclusions of the literature study are found in section A-5.

A-1 Ecological Interface Design

This section will summarize the theoretical fundamentals of the interface design framework known as EID. The interface design framework known as EID is first introduced by Kim J. Vicente and Jens Rasmussen in order to increase safety in process control work domains. This design philosophy is focused on making constrains and relationships in the complex cognitive work domain visible to the end-user, enabling the end-user to limit its core activities to higher order problem solving and decision making. The principles of EID are used in the design of the SSD, and therefore it is of relevance for this project. This section will summarize the development of EID and give an outline for the framework. It is furthermore shown how the theory comes to practice in the design of the SSD.

A-1-1 Development and Relation to Control Theory

When control systems started to evolve towards complex human-machine systems, new design challenges were introduced which led to the development of EID. When identifying these challenges, Vicente and Rasmussen came to a couple of important conclusions, which are listed below (Vicente & Rasmussen, 1992).

1. Three types of events can be classified in complex human-machine systems from the perspective of operators and designers, being:
    (a) Familiar (routine) events
    (b) Unfamiliar, but anticipated events
    (c) Unfamiliar and unanticipated events
2. Two types of human factor problems can be identified, being:
    (a) Anticipated events are more susceptible to slips (i.e. errors of execution)
    (b) Unanticipated events are more susceptible to mistakes (i.e. errors of intention)
3. The interface is inherently bounded to the laws of control:
    (a) Law of Requisite Variety
    (b) Physical systems are described by set of constraints
    (c) Every good controller must possess a model of the to be controlled system

Keeping these observations in mind, Vicente and Rasmussen came up with a structure for the interface design problem as visualized in figure A-1 as is deducted from (Vicente & Rasmussen, 1992).

The interaction between the complex work domain, the interface and the human operator poses two main questions. First, how can the complex work domain complexity best be described? Second, how can the interface best be structured in order to communicate the informational content? This problem structure and the accompanied questions led to the main tools for EID, namely the Abstraction Hierarchy (AH) as described in section A-1-2, which contains the domain representation formalism, and the Skills, Rules & Knowledge (SRK) taxonomy as explained in section A-1-3, containing a model for human behavior dealing with complexity.

A-1-2 Abstraction Hierarchy

In order to perform a proper Work Domain Analysis (WDA) for interface design, Vicente and Rasmussen proposed a 5-level functional decomposition tool called the AH. The AH is used to describe and understand the structure of a system at the following levels of abstraction:

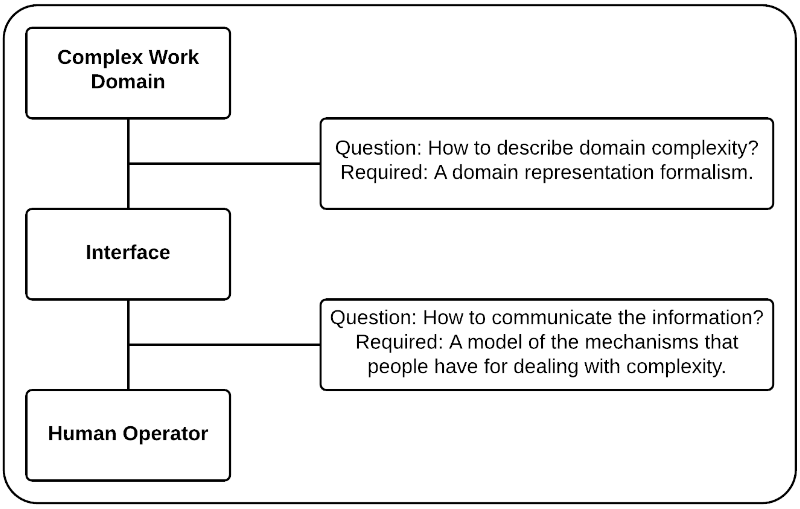

Figure A-1: The structure of the interface design problem

1. **Functional purpose** Contains the generalized goals and purposes of the overall system.
2. **Abstract function** Consists of the laws and principles of physics that are applicable to the system
3. **Generalized function** Explains the complex work domain in terms of standard engineering functions.
4. **Physical function** Represents physical mechanisms associated with the processes.
5. **Physical form** Describes appearance, condition, location and spatial proximity of components.

The top level describes the higher level goals and purposes of the system, while the bottom level describes the physical components of the system. The relationships between the components are indicated by means-ends links (Vicente, 1999) The AH enables the systematical identification of functionally abstract information of a complex work domain, which is a very useful tool in interface design. This is well formulated by St-Cyr et al.: *"An interface that represents the system constraints at multiple levels of abstraction may continue to provide a correct account of the constraints at one level of abstraction when those at another level are violated."* (St-Cyr, Jamieson, & Vicente, 2013)

A-1-3 Skills, Rules & Knowledge Taxonomy

The SRK taxonomy was first developed by Rasmussen in 1983. *"The SRK taxonomy is defined by distinguishing categories of human behavior according to fundamentally different ways of representing the constraints in the environment"* (Vicente, 1999). It is a set of basic distinctions corresponding to a category of human performance, which can be used in the development of human performance models. Each of the three levels represent a different level of cognitive control. Skill-Based Behavior (SBB) level of cognitive control is the basic motor performance of the human body that requires practically no conscious control to perform an action.

Rule-Based Behavior (RBB) uses stored rules known from experience, while not having to understand the underlying principles of the system. In Air Traffic Control (ATC) this RBB is supported by the *"Rules of the Air"* (Annex 2 to the Convention on International Civil Aviation, (ICAO, 2005)), describing a set of rules to avoid collision in conflict situations. When using the SSD, the Air Traffic Controller (ATCo) can use this set of rules when facing unfamiliar, but anticipated events.

Finally, Knowledge-Based Behavior (KBB) comes into play when an unanticipated event occurs. A fundamental understanding of the underlying principles of the system are required in order to perform the right action. Due to the highly complex nature of the air traffic control work domain, there will always be a chance of unanticipated events. Therefore, it is desired for the ATCo to have all required information presented in a logical and integrated manner, such that the controller can apply KBB to focus on problem-solving and decision-making. The cognitive workload is the largest for KBB compared to SBB and RBB.

A-2 Solution Space Diagram

One of the novel ecological interfaces opposed to contribute to the solution of the growing air traffic is called the SSD, developed at the Control & Simulation (C&S) department of the faculty of Aerospace Engineering at Delft University of Technology (DUT). The original SSD developed by Van Dam et al. was designed in order to enable airborne self separation in terms of speed and heading of aircraft in the proximity of conflict situations (Van Dam, Mulder, & Van Paassen, 2008). Later on this was further developed to investigate its use for ATC purposes (Velasco, 2010; Borst, Westin, & Hilburn, 2012).

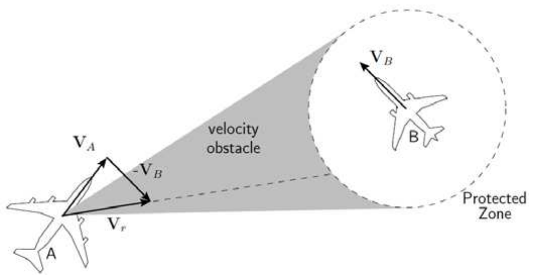

(a) Untranslated conflict zone

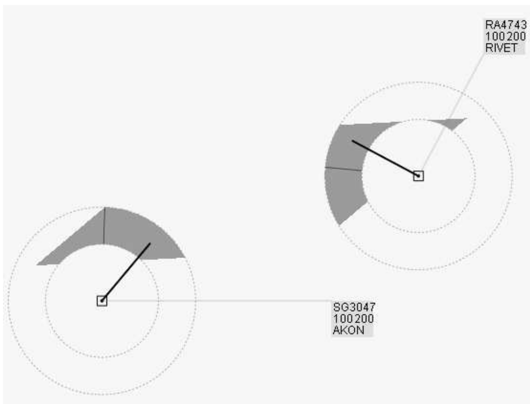

(b) Translated conflict zone in SSD

Figure A-2: Visualization of the SSD

Figure A-2a displays two aircraft, namely aircraft A with velocity vector $\overrightarrow{V_A}$ and aircraft B with velocity vector $\overrightarrow{V_B}$. The Protected Zone of aircraft B (PZ_B) in the horizontal plane is shown as a disk with a 5 NM radius, which is the minimum allowable separation distance for aircraft. Their relative velocity vector $\overrightarrow{V_r}$ of these two aircraft is displayed at the origin of aircraft A, indicating how aircraft A moves with respect to aircraft B. Using this visualization, it can instantly be seen that when $\overrightarrow{V_r}$ moves in the direction of PZ_B a loss of separation will occur. In fact, any combination of $\overrightarrow{V_A}$ and $\overrightarrow{V_B}$ such that $\overrightarrow{V_r}$ is located in the grey colored triangle called the Forbidden Beam Zone (FBZ), leads to a loss of separation.

Figure A-2b shows exactly the same traffic situation, this time with the FBZ translated by velocity vector of the other aircraft and represented as in the SSD interface. In this case, the velocity vector is indicated by the thick black lines, indicating both the magnitude and direction of the velocity. The inner and outer circles indicated in the SSD visualization represent the minimum and maximum velocities of the aircraft. Now assume that aircraft A is the controlled aircraft, and aircraft B is the observed aircraft, meaning that an air traffic controller can redirect the controlled aircraft by giving velocity and heading commands. The SSD of the controlled aircraft shows its solution space in terms of velocity and heading at the current velocity and heading of the observed aircraft. As can be clearly seen from figure A-2b, the current velocity vectors of each aircraft are in the FBZ of the other aircraft and over time this will ensure a loss of separation if no action is taken. Therefore, the controlled aircraft must modify its absolute speed vector outside the FBZ, i.e. the white space of the SSD. It is clear that the SSD only offers solutions in the horizontal plane, since it is not considering the vertical solution space. The main conclusion of the experiment performed by Borst et al. is that novices found the SSD useful and were eager to react to red conflict warnings and experienced controllers were more skeptic towards the SSD (Borst et al., 2012). This version of the SSD is used in the conducted preliminary experiment.

A-3 Sensor Fault Diagnosis & EID

In order to implement the EID philosophy to an industry-wide application, several obstacles have to be conquered. In order to control a complex system, sensors are used to collect and display information about the state of the work domain on the interface. Configuring and visualizing these individual variables in a organized and logical way will create emergent features, indicating significant task-relevant variables that can be used for higher-order problem solving and decision making. This ecological way of representing the control problem should reduce the cognitive workload of the operator, since the useful variables are integrated in the display and do not need to be derived from lower-level sensors.

One of the greatest concerns thus far is the effect that noisy or faulty sensors have on operator performance. The hypothesis on this specific topic is two-fold. On the one hand, it can be reasoned that an EID interface should be resilient against incorrect sensor information due to explicit representation of the redundant constraints by the means-ends links as modeled in the AH. On the other hand, it can be argued that system operators would easily confuse the displayed state of the work domain with the actual state, *because* the constraints are visualized and easy to perceive (Vicente et al., 1996; Vicente, 2002).

The different visions of both EID and control theorists on sensor fault diagnosis are elaborated on in section A-3-1. There has been some previous research in the field of the robustness of system performance using an interface designed according to the EID principles.

A-3-1 Analytical Redundancy

The main difference between the EID approach on sensor fault detection and the approach of classical control theorists is the human factor. Several analytical models for fault detection have been developed, based on parity equations, parameter estimation and state estimation methods (Isermann, 1997; Frank, 1990). By comparing an analytical reference model to the actual state of the system, an unexpected deviation of the residual can lead to a sensor fault detection and diagnosis (Vicente & Rasmussen, 1992).

In EID, these analytical tools can be used and implemented in the interface as a means such that the operator can make a well-informed decision on sensor fault diagnosis, meaning that the operator remains responsible. The idea is that if the higher-order functional constraints are explicitly visualized in the interface, it should be easier for the system operator to identify broken constraints, i.e. diagnose a faulty sensor. It should be noted that this also depends on the interpretation of the operator. By making a proper WDA of the controlled system using and AH the designer is able to identify the information necessary for operators to deal with the complete working spectrum of the system, including unanticipated events.

Control theorists however argue that fault diagnosis should be completely automated using these analytical models. The fear is that human factors will cause faulty sensors to be overlooked. However, such a model will only account for familiar and anticipated events. When an unfamiliar and unanticipated event will occur, the analytical reference model might be inadequate to detect and diagnose sensor failure. Therefore in EID it is believed that the human capacity in the sense of adaptability, creativity and flexibility plays a crucial role in decision making in control problems. These cognitive capabilities activated during KBB are crucial in the complex work domain of human-machine systems.

The current version of the hypothetical SSD tool does not include an analytical redundancy model for detection of sensor failure. In order to integrate such a tool, a reference model of the system should be designed that is able to accurately simulate and predict the normal system behavior. Therefore in the experiments conducted for this research, the participants are not aided by such redundancy tools. The subjects can only rely on the integrated information presented on the interface.

A-3-2 Previous Research

This section discusses briefly the conclusions of several investigations towards sensor failure in systems using interfaces designed according to the EID principles.

DURESS III An experiment conducted using a thermal-hydraulic process simulation called the DUal Reservoir Simulation (DURESS) III studied the effect of sensor failure between EID and Single-Sensor Single-Indicator (SSSI) interfaces. Results showed that there was no significant influence of increasing sensor failure on the performance and control stability of EID operators. In fact, the performance and control stability of the participants using the EID was not inferior to that of the SSSI interface. (St-Cyr, 2006a, 2006b; St-Cyr et al., 2013)

Pasteurizer II Research done by Reising and Sanderson involving a micro world process pasteurization control system called the Pasteurizer II consisted of an experiment investigating the differences of an EID interface over the conventional Piping-and-Instrumentation Diagram (PID) for minimal and maximal adequate instrumentation set-up. It showed that the maximally adequate EID interface showed the best failure diagnosis performance over the conventional PID. The main conclusion drawn in this research that interfaces should display all relevant information to the operator, which becomes crucial in unanticipated events like sensor failures (Reising & Sanderson, 2004). This is indeed in accordance with the Law of Requisite Variety, implying that an interface should not trivialize the control problem but instead it should reflect the complete solution space, as is the case in the SSD. This will increase the capacity of the system to move within that problem space.

Synthetic Vision Display Finally, Borst et al. did research towards sensor failure in an avionic application called the Synthetic Vision Display (SVD). This tool provides the pilot with a computer generated perspective view of the surrounding terrain environment, integrated into the primary flight status information visualization. The purpose of the SVD is to give the pilot enhanced terrain awareness, which is visualized in figure A-3 (Borst, Mulder, & Van Paassen, 2010).

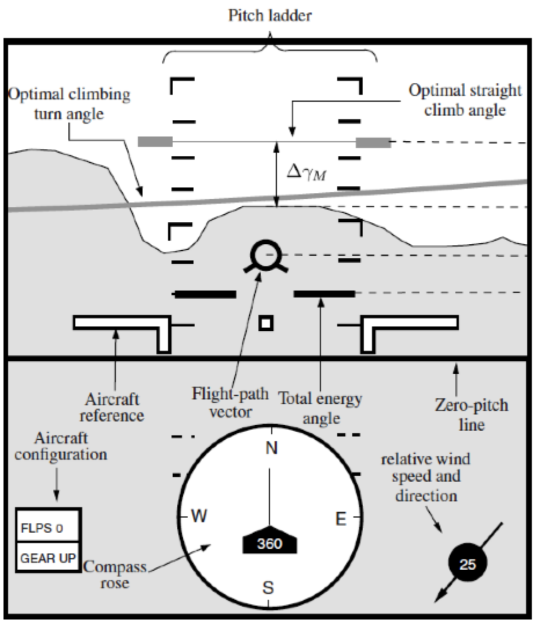

Figure A-3: Schematic drawing of the Synthetic View Display for enhanced terrain awareness

Two versions of the SVD were tested, namely the baseline version showing only lower-order work domain elements, and the ecological SVD variant showing higher-order functional details of the complex work domain. One of the main conclusions of the experiment was that malfunctioning flaps and engines became more obvious using the constraint-based ecological SVD, supporting the EID principles (Borst et al., 2010). Furthermore, the ecological SVD led to an improved pilot terrain awareness but also a higher workload. It can be deducted from this research that it might be desirable for the operator to stay actively involved in the control process rather than to let automation solve the control problem.

Industry-Scale Research In an industry-scale research project on a petrochemical process control, Jamieson et al. conducted an experiment on a large group of professional operators to indicate the difference in performance between ecological interfaces and contemporary displays. Overall operator performance of the ecological interface turned out the be far better in terms of faster trial completion times, more accurate fault diagnoses, and more effective control responses (Jamieson, 2003).

A study conducted by Burns et al. investigated the influence of spatial and temporal proximity of related information objects on fault detection and diagnosis. The work domain used for evaluation was a simulation of an industry-scale conventional coal-fired powerplant, with 402 plant variables. Results showed that spatial proximity on its own has an positive effect on the sensor fault detection time, and in combination with temporal proximity improved the sensor fault diagnosis. This was in accordance with the hypothesis that maximal integration in space and time along means-end links improves operator problem solving (Burns, 2000).

In order to test the sensor fault detection and diagnosis performance between the different levels of the AH, Ham et al. compared three displays for the control of a secondary cooling system of a pressurized water reactor nuclear power plant. The first display only indicated generalized function information with the physical information, the second display showed additionally the abstract function information, and the third display also visualized the means-ends relations between the different levels of abstraction. Results of this experiment showed that the display with AF-level information showed increased efficiency compared to a display showing only GF-level information, specifically in cognitive demanding situations. Adding the explicit representation of means-ends links in the third display significantly increased operator performance. This indicated that showing information at a higher abstraction level and visualizing the means-ends relations results in a improved awareness of the system, which helps the operator significantly with problem solving in unexpected situations (Ham & Yoon, 2001). One important lesson from the research of Ham et al. that is of relevance for this experiment is that enabling an explicit representation of the means-ends relations led to increased operator performance.

A-4 ADS-B reliability

For this experiment the SSD interface uses two sensors to construct an image of the current traffic situation, namely the Primary Radar (PR) and ADS-B. Since the project will focus on sensor failure, it is of importance to better understand where the information is coming from, and what realistic errors are, which is discussed in this section.

The basis of the future surveillance system will be a system called ADS-B, which will be supplemented by the already existing PR and Secondary Surveillance Radar (SSR). It is a cooperative dependent surveillance technology, where aircraft avionics will broadcast information to ATC and other nearby aircraft, containing among others information like the latitude, longitude, velocity, altitude, transponder code and aircraft's call sign. This transmitted information is dependent on the aircraft navigation equipment (e.g. Global Positioning System (GPS), Inertial Navigation System (INS), etc) and therefore the reliability of these onboard avionics is crucial to the success of ADS-B. The system also includes a data link, enabling ground-to-air communication like weather data and airspace status information.

Source	**Availability (FOM≥4) [%]**	**Latency (Avg.) [s]**	**Horizontal position accuracy [m]**	**Update rate [s]**
1	81.6	0.5567-1.9050	RMS: 30.8691-14287	1.0-9.6
2	99.96	95%:2.8 99.65% :<10	RMS: 254	79.97%:1 12.50%:2 3.55%:3 3.98%:higher
3	98.91	95%: < 1.5 99.9% :<3	< 926 in 95%	N/A
4	89.76	N/A	33-300	N/A
5	60	N/A	N/A	N/A

Table A-1: ADS-B Reliability Summary

In order to construct a representational simulation, it is therefore necessary to find out what realistic ADS-B sensor failures and inaccuracies are. Therefore it should be fully understood how ADS-B works, what the potential threats are, what frequently occurring errors are and how this can be integrated in the experiment. An initial reliability study already showed significant latencies and horizontal position inaccuracies with ADS-B in practice, further indicating the significance of this research (Torel, 2014). The reliabilities found from several studies are summarized in table A-1 and show serious discrepancies.

Table A-1 shows the results of five recent research projects on the performance of ADS-B systems. The research has been done in the following areas:

1. London TMA (Ali, Majumdar, Ochieng, & Schuster, 2013)
2. Several Southern European air navigation service providers (Cedrini et al., 2010)
3. Ground stations spread around Europe (Rekkas & Rees, 2008)
    - EUROCONTROL Experimental Centre (EEC), Bretigny, France
    - Toulouse (DSNA), France
    - Langen (DFS), Germany
    - Athens (HCAA), Greece
    - Schiphol (LVNL), Netherlands
    - Walingham (NATS), UK
4. Route Chengdu to Jiuzhai, China (Zhang, Liu, & Zhu, 2011)
5. Beijing FIR region, China (ICAO, 2013)

A-5 Conclusions

The interface design framework known as EID is used in the development of the SSD, which aims at supporting controllers at their Conflict Detection & Resolution (CD&R) task. Previous research on sensor failure in EID show that operators are positively supported by interfaces designed according to the EID framework that explicitly represent the constraints of the control problem in the case of failure diagnosis. Even though these research projects show some empirical evidence in favor of EID, there is still a lot of work to be done. So far there has not been any research in this field for the SSD ecological interface. Therefore, an extensive research must be done and an experiment must be executed in order to prove that the EID principles are implemented correctly and operator behavior will be conform the expectations in the case of sensor failure diagnosis. If this turns out not to be the case, the results might imply that crucial constraints identified by the AH are not sufficiently well represented in the interface, and some adjustments to the tool should be recommended. The results from the ADS-B performance studies show that ADS-B is not reliable enough as a sole means for surveillance.

Appendix B

SSD Sensitivity Analysis

This appendix presents the calculations performed to determine the sensitivity of the SSD. The FBZ width angle is of most importance since it indicates the distance to the observed aircraft, see figure B-1.

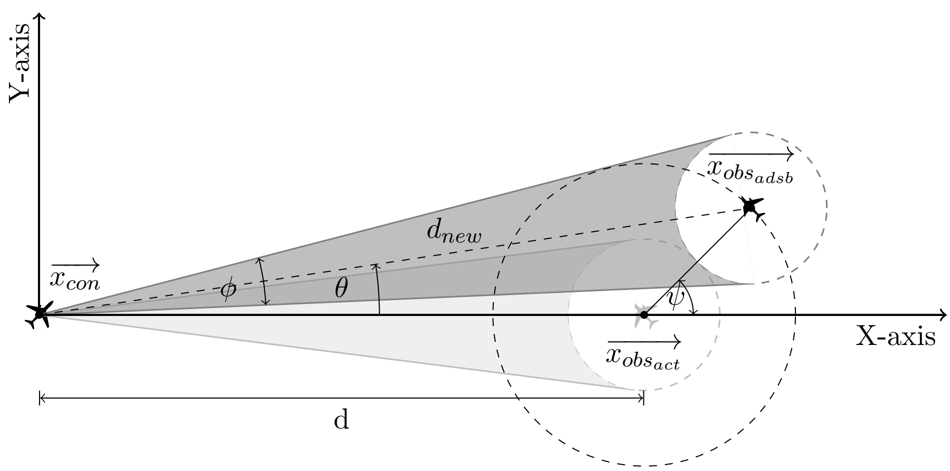

Figure B-1: Sensitivity analysis geometry

First, the distance between $\overrightarrow{x}_{con}$ and $\overrightarrow{x}_{obs_{act}}$ is determined using equation B-1.

$$d = \sqrt{(x_{obs_{act}} - (x_{con})^2 + (y_{obs_{act}} - (y_{con})^2} \tag{B-1}$$

The location of $\overrightarrow{x}_{obs_{adsb}}$ is then found using equation B-2.

$$\overrightarrow{x_{obs_{adsb}}} = \begin{bmatrix} x_{obs_{adsb}} \\ y_{obs_{adsb}} \end{bmatrix} = \begin{bmatrix} x_{obs_{act}} + \varepsilon * cos(\psi) \\ y_{obs_{act}} + \varepsilon * sin(\psi) \end{bmatrix} \tag{B-2}$$

Here, the error distance is indicated by ε, and is set to 10NM for this analysis. From these equations, the new distance d_{new} can be determined using equation B-3.

$$d_{new} = \sqrt{(x_{obs_{adsb}} - x_{con})^2 + (y_{obs_{adsb}} - y_{obs_{con}})^2} \tag{B-3}$$

The FBZ width angle ϕ can then be calculated with equation B-4.

$$\phi = 2sin^{-1}\left(\frac{R_{PZ}}{d_{new}}\right) \tag{B-4}$$

Here, R_{PZ} indicates the radius of the protected zone, which for en-route flight is considered 5NM. The results are shown in figure B-2.

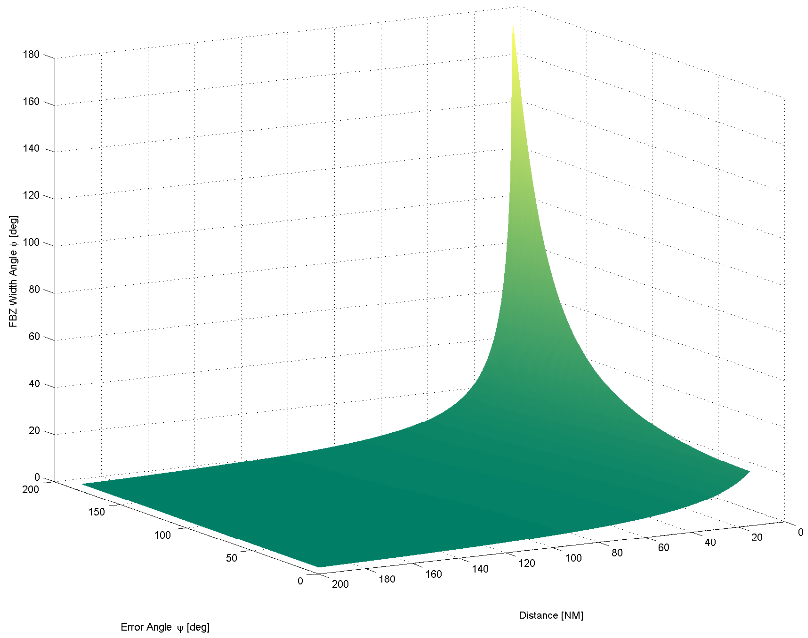

Figure B-2: Forbidden Beam Zone width angles for various distances and error angles

Furthermore, the FBZ radial angle θ is determined using formula B-5.

$$\theta = tan^{-1}\left(\frac{y_{obs_{adsb}}}{x_{obs_{adsb}}}\right) = sin^{-1}\left(\frac{y_{obs_{act}} + \varepsilon * sin(\psi)}{x_{obs_{act}} + \varepsilon * cos(\psi)}\right) \tag{B-5}$$

The results are shown in figure B-3.

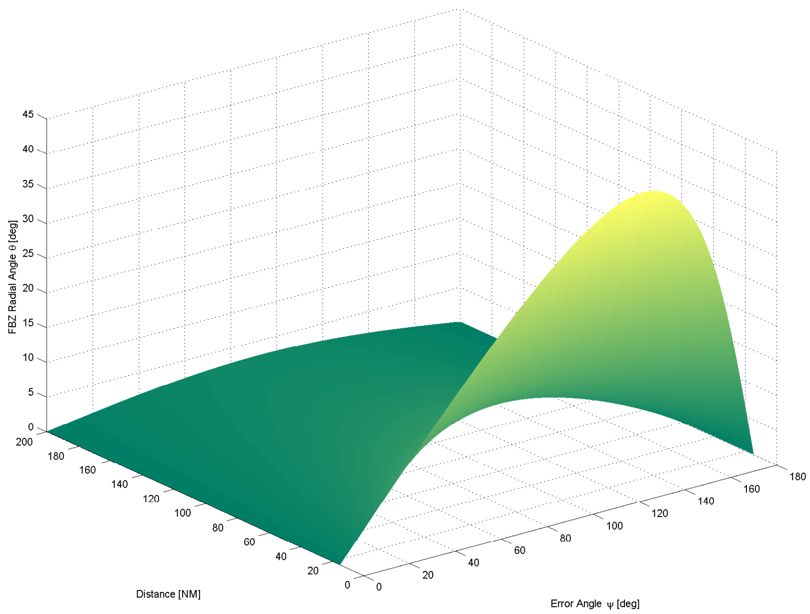

Figure B-3: Forbidden Beam Zone radial angles for various distances and error angles

Appendix C

Experiment Briefing

This document will give a short introduction to an experiment conducted in the Air Traffic Management (ATM) Lab. After reading this document the participant should have a reasonable understanding of the experiment. At the beginning of the experiment the participant will receive a training session to familiarize with the Solution Space Diagram (SSD) tool.

Goal of the experiment

Ecological Interface Design (EID) is a design framework used in the development of the SSD, a hypothetical Conflict Detection & Resolution (CD&R) tool for Air Traffic Control (ATC) developed at Delft University of Technology (DUT), as is depicted in figure C-1. For this hypothetical experiment, the SSD interface is constructed from information of both Primary Radar (PR) and Automatic Dependent Surveillance Broadcast (ADSB) to form an image of the traffic situation and to determine the solution space for aircraft in conflict. The aim of this research is to evaluate the performance of the controller using the SSD.

Your participation is completely voluntary and you have the right to withdraw from the study at any moment without explanation. The recorded data are made anonymous, and are to be used solely for academic and project-related purposes.

Apparatus

The experiment will be conducted in the ATM Lab located on the second floor inside the SIMONA building, room SIM 2.03. The SSD simulation will take place in the MUFASA simulation environment. The participant can interact with the simulator using a regular mouse and keyboard.

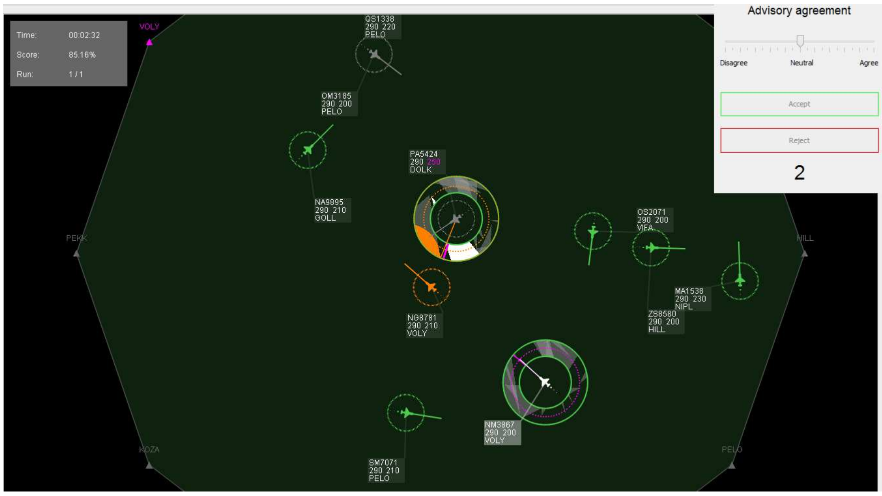

Figure C-1: Impression of the Solution-Space Diagram.

Controller task

The primary controller task is to secure safe separation of aircraft by resolving emerging conflicts. The secondary controller task is to ensure all aircraft leave the sector at their designated exit point (COPx). It can do so by accepting or declining advisories, and subsequently the controller can manually command resolutions to those aircraft if necessary. It is stressed out to the participant to carefully check the SSD for correctness before applying any resolution.

Procedure

The experiment will start with a briefing in combination with training run in which the basic working principles of the interface will be discussed. This includes an explanation and demonstration of the SSD, showing how geometries form and change in the interface. The training scenarios gradually build up in complexity to the level of the actual test scenarios. The briefing ends when the controller has indicated to have a good understanding of the interface and the experiment, and does not need to practice with more training scenarios.

After the briefing and a short break, the participant will be engaged in 14 scenarios of about three minutes over two rounds, where experimental conditions occur in random order. The participant can initiate the scenario when ready. After each scenario the participant should fill in the workload score. The participant is encouraged to verbally communicate with the supervisor in the case of comments on the scenario.

When the experiment is finished and the data is collected, a debriefing will take place, at which point the participant is encouraged to give comments, feedback or just share their experiences. An overview of the experiment activities can be found in table C-1.

Activity	Introduction	Training	Break	Round 1	Break	Round 2	Debriefing
Duration	5 min	40 min	10 min	40 min	10 min	40 min	5 min

Table C-1: Experiment Timeline.

Appendix D

Verbal Briefing Protocol

Introduction The SSD is CD&R tool for ATC, and it uses information from both ADS-B and PR.

The untranslated conflict zone (see information chart) shows a controlled aircraft A and an observed aircraft B with different velocities and Protected Zone (PZ). A FBZ is defined by the area formed by the tangent lines between the PZ and the origin of aircraft A. If the relative velocity is in this FBZ a conflict exists and a LoS will occur in future if no actions are taken.

The translated conflict zone shows the same situation with FBZ translated by velocity vector of the observed aircraft. Two circles indicate the minimum and maximum speed of the controlled aircraft. Note that the tip of the bisector of the FBZ starts at the velocity vector of the observed aircraft, and the cone faces towards that aircraft. The further away the aircraft, the narrower the FBZ width angle.

See actual interface visualization (information chart) showing controlled aircraft and explain all lines, circles and colors in SSD as described on chart.

Explain aircraft label and input controls according to information chart (ONLY EXPLAIN TO MEANS-ENDS FUNCTIONALITY TO GROUP II!).

The first five training scenarios will be passive and explanatory. After that the training scenarios will be active and the participant is engaged as an air traffic controller.

T1: Lay-out and SSD basics Explain controlled sector, its boundaries, the designated exit points, and that only aircraft inside sector can be controlled. Explain symbols, labels (ACID, Speed, Altitude, COPx), color codes, simulator time, score (deviation from exit, red alert conflict) and number of runs. Explain formation of FBZ in SSD and which commands lead to conflict between controlled and observed aircraft.

T2: Distance between aircraft Explain how distance between controlled and observed aircraft changes the width of the FBZ. Further away means a smaller FBZ width angle, closer means a larger FBZ width angle, whilst the origin of the FBZ stays on the same location, namely the tip of the bisector.

T3: Multiple aircraft in line Explain how multiple FBZ's can overlap when aircraft are in line. Therefore it is not possible to distinguish the narrow FBZ of the furthest observed aircraft from the wide FBZ of the closest observed aircraft.

(ONLY FOR GROUP II MEANS-ENDS ON: Explain that by hovering and right mouse clicking aircraft in conflict are highlighted)

T4: Heading Explain how changing the heading of one aircraft changes the origin of the FBZ of the other aircraft, whilst the SSD of the aircraft with changed heading stays the same.

T5: Location Explain how changing the location of one aircraft changes the orientation of the FBZ of both aircraft, whilst the origin of the FBZ stays the same.

T6: Advisory Explain that advisory is given by orange line indicating both heading and velocity. The participant has 30 seconds to respond, otherwise it will automatically be implemented. Before responding, the participant has to indicate an agreement rating to enable activation.

T7: Manual command After agreeing, declining or expiring an advisory, the participant can manually give a alternative command by clicking (heading), scrolling (velocity) and pressing enter (confirm).

Controller task The primary controller task is to secure safe separation of aircraft. The secondary controller task is to ensure all aircraft leave the sector at their designated exit point (COPx). This can be done by accepting or declining advisories, and subsequently the controller can manually command resolutions to those aircraft. It is emphasized to the participant to carefully check the SSD for correctness before applying any resolution. As mentioned before, the SSD uses information from PR and ADS-B. In the case of doubt, the participant should use his best judgment and act accordingly within the options available.

T8-T11: Resolve conflicts Participant must use all current knowledge to solve conflicts, but they also have to try to let the aircraft leave at the desired COPx. Emphasize that they must always check the SSD of the aircraft in conflict for correctness before applying a command.

Questions and extra training Ask if participant feels acquainted with the interface. Ask if anything is unclear. Ask if the participant wants more training scenarios. When actual test scenarios start, the experiment conductor can not communicate with the participant anymore. Encourage the participant to verbally communicate its interpretation of the scenario and its reasoning of activities throughout all scenarios of the experiment.

Appendix E

Experiment Information Chart

INFORMATION CHART

VISUALIZATION

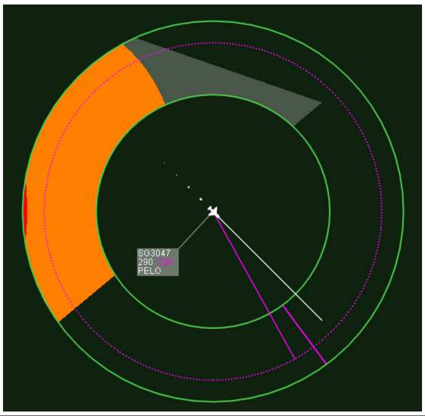

GREEN CIRCLES:	MIN/MAX SPEED
WHITE LINE	CURRENT SPEED/HEADING
PURPLE CIRCLE:	SELECTED SPEED
THIN PURPLE LINE:	SELECTED SPEED/HEADING
THICK PURPLE LINE:	EXIT POINT (COPX)
GREY TRIANGLE:	FORBIDDEN BEAM ZONE
ORANGE AREA:	FORBIDDEN BEAM ZONE
RED AREA:	FORBIDDEN BEAM ZONE
GREY SQUARE:	AIRCRAFT LABEL

AIRCRAFT LABEL

AIRCRAFT CALL SIGN

FLIGHT LEVEL (FL) CURRENT SPEED

EXIT POINT (COPX)

INPUT CONTROLS

LEFT MOUSE CLICK	A/C SSD INSPECTION
CTRL + LEFT MOUSE CLICK	MOVE OVER SCREEN
CTRL + SCROLL WHEEL	ZOOM IN/OUT
SCROLL WHEEL IN CONTROLLED A/C	CHANGE DESIRED SPEED
ENTERED IN CONTROLLED A/C	APPROVE SPEED/HEADING COMMAND

INFORMATION CHART

SSD FORMATION

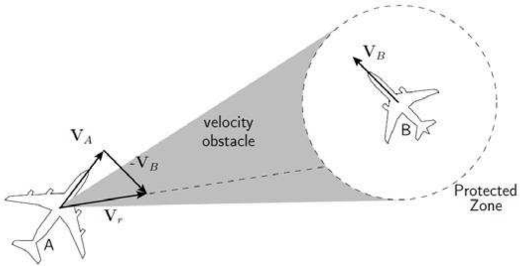

UNTRANSLATED CONFLICT ZONE

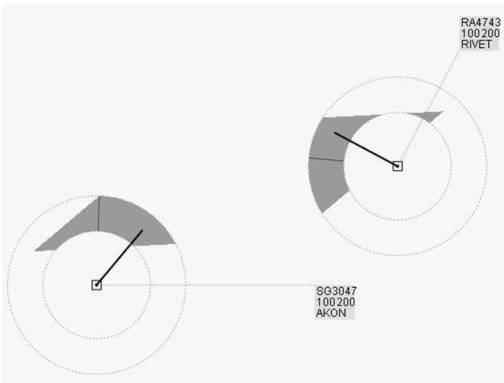

TRANSLATED CONFLICT ZONE

Appendix F

Experiment Setup

This appendix presents the design of the experiment, showing the order in which the of the measurement runs were executed. Three independent variables were tested, namely means-ends relations off (**group I**) and on (**group II**), complexity low (**L**) and high (**H**), and sensor failure absent (**N**) and present (**Y**), resulting in four basic scenarios (**A:LxN**, **B:LxY**, **HxN**, and **HxY**). Two repetitions of each scenario were taken, where the scenarios would be rotated 180 degrees to prevent recognition of the scenarios. Between the repetitions, a coffee break of approximately 15 minutes was held to refresh the participants attention. Furthermore, there was some difference in experience in ATC within the pool of participants. They were therefore spread out evenly over group I (means-ends disabled) and group II (means-ends enabled). Dummy runs were incorporated in random order between the actual measurement runs to prevent further recognition of scenarios and traffic geometries.

	Conditions															
Scenario	A:LxN	B:LxY	A:LxN	B:LxY	C:HxN	D:HxY	C:HxN	D:HxY	A:LxN	B:LxY	A:LxN	B:LxY	C:HxN	D:HxY	C:HxN	D:HxY
Letter	A	B	C	D	E	F	G	H	I	J	K	L	M	N	O	P
ME	Off	Off	Off	Off	Off	Off	Off	Off	On	On	On	On	On	On	On	On
Complexity	Low	Low	Low	Low	High	High	High	High	Low	Low	Low	Low	High	High	High	High
Rotation	0	0	180	180	0	0	180	180	0	0	180	180	0	0	180	180
Failure	Off	On	Off	On	Off	On	Off	On	Off	On	Off	On	Off	On	Off	On

	MORE EXPERIENCED								LESS EXPERIENCED							
	Group I: ME Off				**Group II: ME On**				**Group I: ME Off**				**Group II: ME On**			
	1	2	3	4	5	6	7	8	9	10	11	12	13	14	15	16
Repetition I	A	D	H	E	I	L	P	M	A	D	H	E	I	L	P	M
	Dummy Run				Dummy Run				Dummy Run				Dummy Run			
	D	H	E	A	L	P	M	I	D	H	E	A	L	P	M	I
	Dummy Run				Dummy Run				Dummy Run				Dummy Run			
	E	A	D	H	M	I	L	P	E	A	D	H	M	I	L	P
	Dummy Run				Dummy Run				Dummy Run				Dummy Run			
	H	E	A	D	P	M	I	L	H	E	A	D	P	M	I	L
	BREAK								BREAK							
Repetition II	B	C	G	F	J	K	O	N	B	C	G	F	J	K	O	N
	Dummy Run				Dummy Run				Dummy Run				Dummy Run			
	F	B	C	G	N	J	K	O	F	B	C	G	N	J	K	O
	Dummy Run				Dummy Run				Dummy Run				Dummy Run			
	C	G	F	B	K	O	N	J	C	G	F	B	K	O	N	J
	Dummy Run				Dummy Run				Dummy Run				Dummy Run			
	G	F	B	C	O	N	J	K	G	F	B	C	O	N	J	K

Appendix G

Additional Experiment Results and Statistics

This appendix presents additional plots obtained from the experiment.

Additional Experiment Results

Figure G-1 shows additional experimental data. Figure G-1a shows the cumulative number of incorrect accepted advisories, and as can be seen the total number is for both cases lower if the means-ends relations are enabled. A Kruskal-Wallis test showed that this difference in distributions is insignificant. Furthermore, it can be seen that a higher complexity seems to result in a higher number of incorrect accepted advisories. This is confirmed by a Friedman test ($\chi^2(1) = 4.455, p = 0.035$).

Figure G-1b shows the cumulative number of incorrect rejected advisories. It can be seen that the total number lies much lower than for the incorrect accepted advisories, indicating a relatively high automation acceptance in incorrect situations, and a lower automation rejection behavior in correct situations. No trend can be seen from the figures, which is confirmed by statistical tests.

The number of manual heading commands are recorded and the cumulative numbers are plotted in Figure G-1c. There seem to be a trend between sensor failure presence, however there is no indication for effects of group or complexity. This initial analysis by looking at Figure G-1c is confirmed by statistical tests. No significance is found between groups, but a Friedman test ($\chi^2(3) = 23.180, p < 0.001$) followed by a Wilcoxon Signed Ranks test show pairwise differences in distributions for scenarios A-B (Z=-2.989, P=0.003), A-D ($Z = -3.191, P = 0.001$), B-C ($Z = -2.847, P = 0.004$), C-D ($Z = -3.265, P = 0.001$), indicating that heading commands are significantly more frequently used in the presence of a failure.

The number of manual speed commands are recorded and the cumulative numbers are plotted in Figure G-1d. Statistical tests indicate that there are no significant different distributions.

The number of manual combined speed and heading commands are recorded and the cumulative numbers are plotted in Figure G-1e. Again, there seems to be a small trend for sensor failure presence, where a presence leads to a higher number of manual combined commands. A Kruskal-Wallis test shows that only for scenario C:HxN there is a significant difference between groups ($\chi^2(1) = 5.067, p = 0.024$) on the number of combined commands given. A Friedman test ($\chi^2(3) = 29.940, p < 0.001$) followed by a Wilcoxon pairwise comparison shows differences between the following scenarios: A-B ($Z = -3.525, P < 0.001$), A-D ($Z = -3.421, P = 0.001$), B-C ($Z = -2.935, P = 0.003$), C-D ($Z = -2.794, P = 0.005$). This clearly indicates that in the presence of a sensor failure, more combined manual commands are given.

The cumulative number of intrusions is plotted in Figure G-1f. It can be seen that overall the group with the means-ends relations had fewer intrusions, however the distributions were not significantly different. Also no effect of complexity on the number of intrusions was found.

Furthermore, Figures G-2, G-3 and G-4 show the Q-Q plots for the agreement rating, workload and response time, respectively. These are used to check if the samples can be considered normally distributed, which was the case for these three dependent measures. It should be noted that the sample size per group of eight is relatively small, therefore not every slight deviation from the linear curve are directly an indication of non-normality. A larger sample size would smooth this out. Even though some plots are slightly skewed (Figures G-2f, G-4b and G-4f), overall they can be considered to be approximately normally distributed and qualified for an ANOVA test.

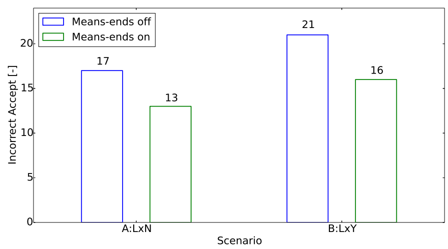

(a) Incorrect accepted advisories.

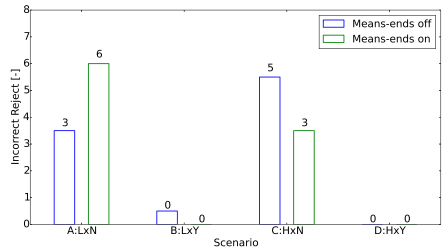

(b) Incorrect rejected advisories.

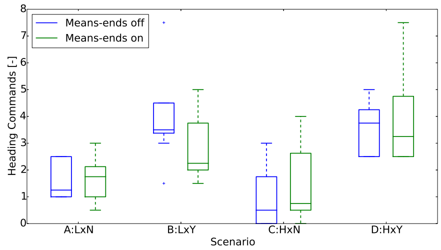

(c) Manual heading commands.

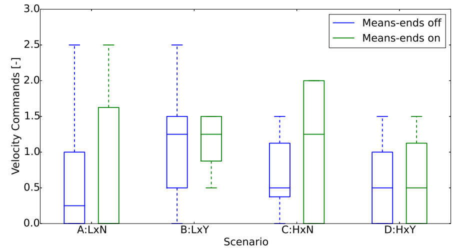

(d) Manual velocity commands..

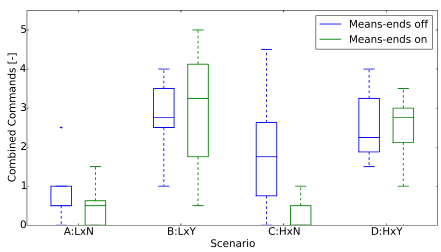

(e) Manual combined commands.

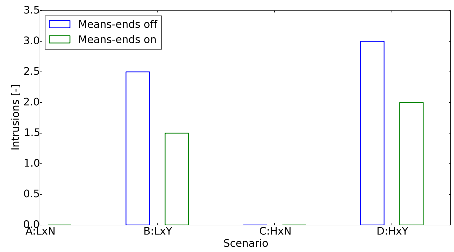

(f) Number of intrusions.

Figure G-1: Additional experiment data.

Normalized Agreement Ratings Q-Q Normality Plots

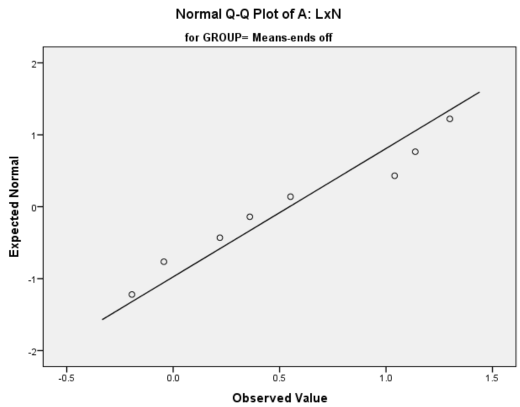

(a) A:LxN group I.

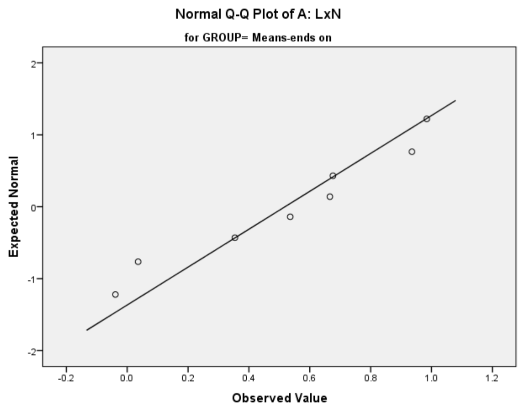

(b) A:LxN group II.

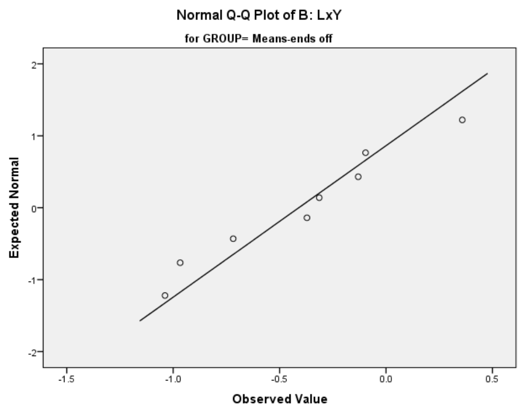

(c) B:LxY group I.

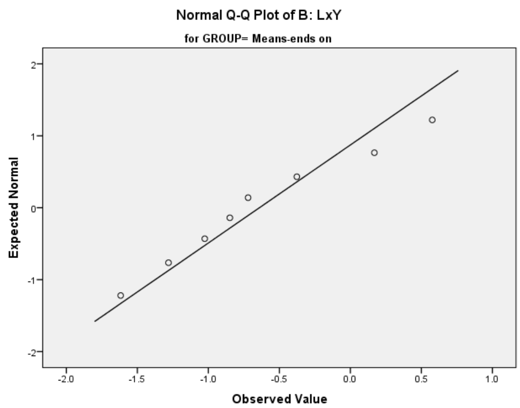

(d) B:LxY group II.

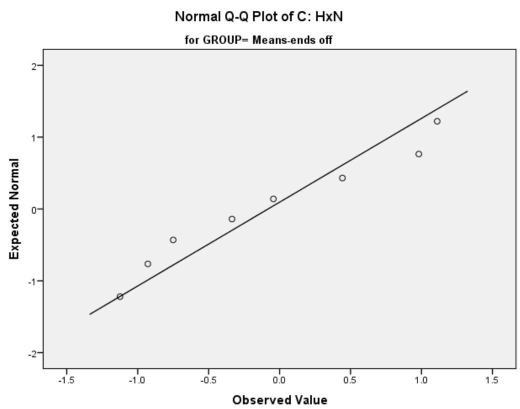

(e) C:HxN group I.

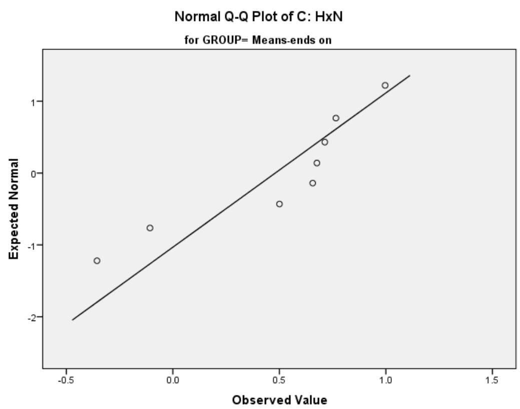

(f) C:HxN group II.

Figure G-2: Normalized agreement ratings Q-Q normality plot.

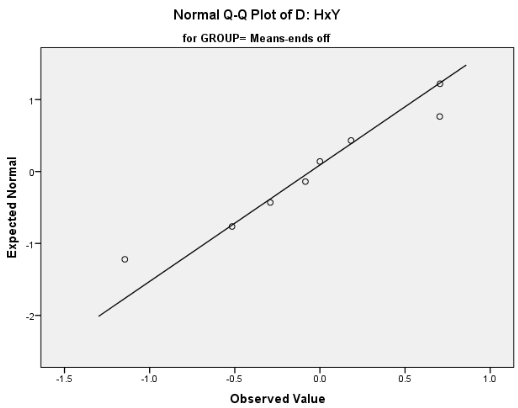

(g) D:HxY group I.

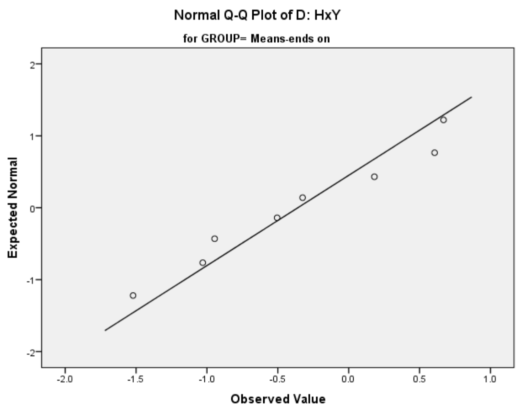

(h) D:HxY group II.

Figure G-2: (Cont.) Normalized agreement ratings Q-Q normality plot.

Normalized Workload Q-Q Normality Plots

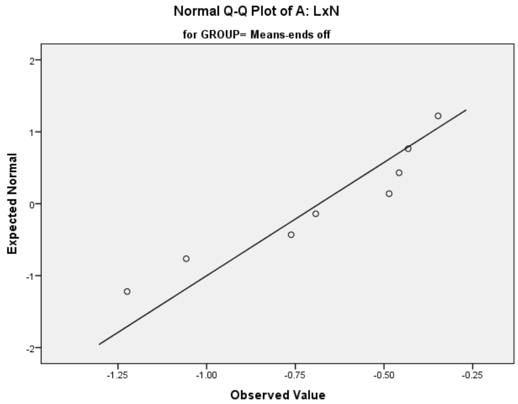

(a) A:LxN group I.

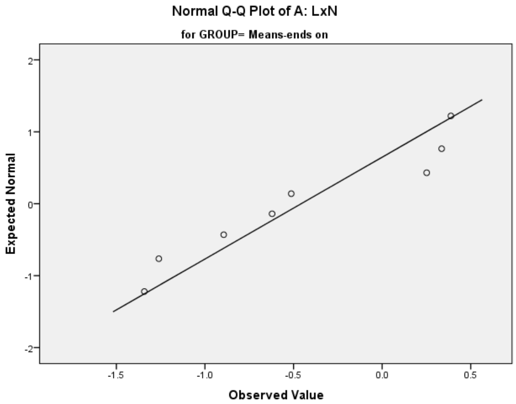

(b) A:LxN group II.

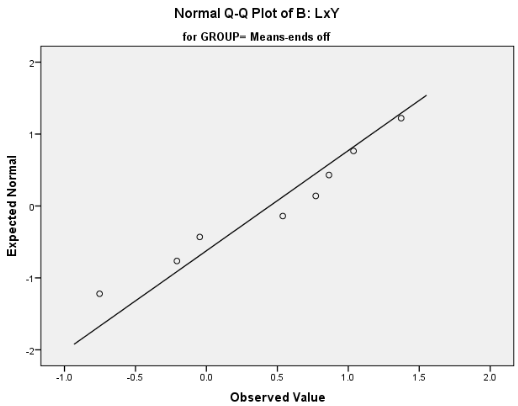

(c) B:LxY group I.

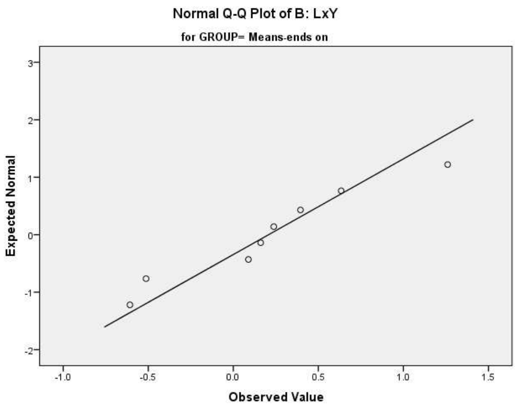

(d) B:LxY group II.

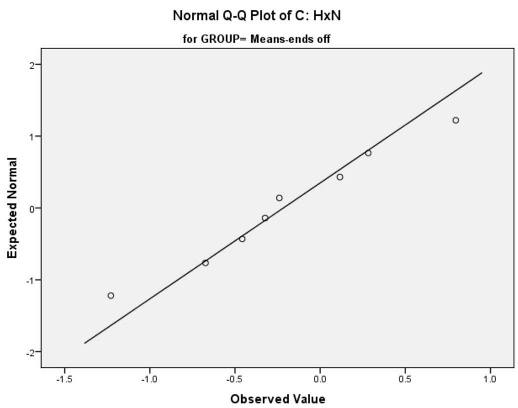

(e) C:HxN group I.

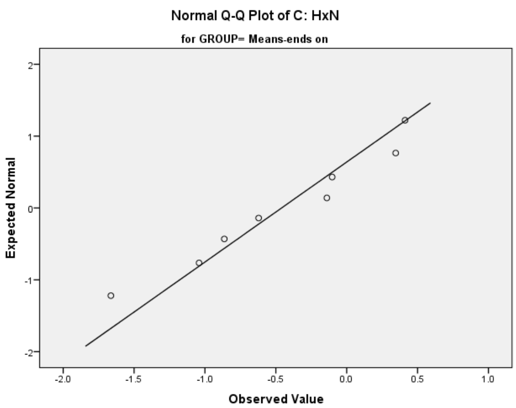

(f) C:HxN group II.

Figure G-3: Normalized workload Q-Q normality plot.

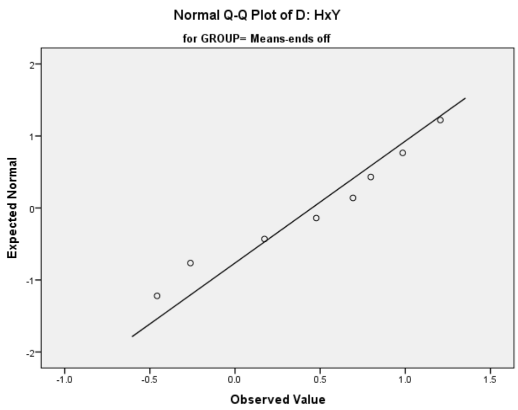

(g) D:HxY group I.

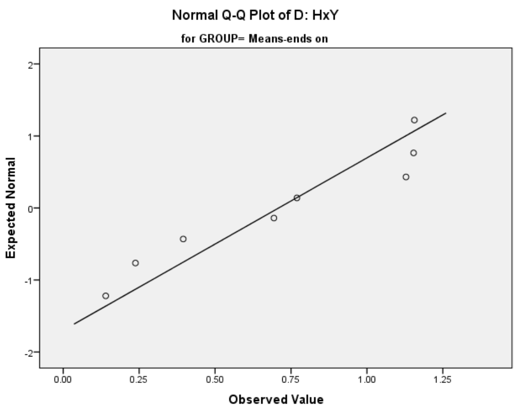

(h) D:HxY group II.

Figure G-3: (Cont.) Normalized workload Q-Q normality plot.

Advisory Response Time Q-Q Normality Plots

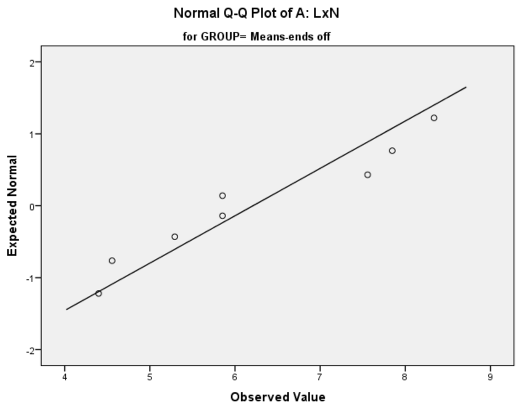

(a) A:LxN group I.

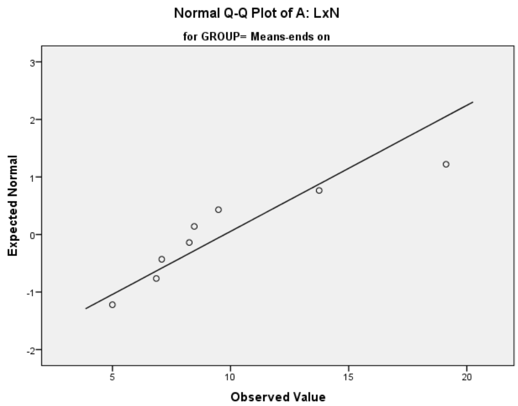

(b) A:LxN group II.

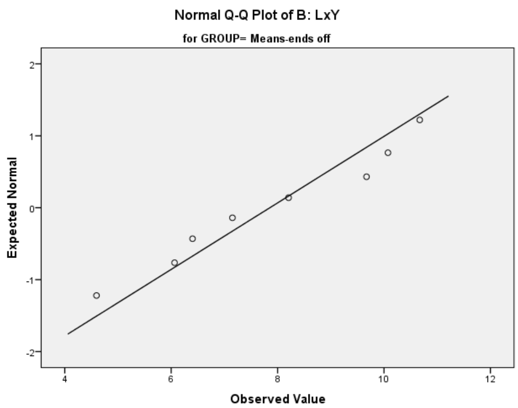

(c) B:LxY group I.

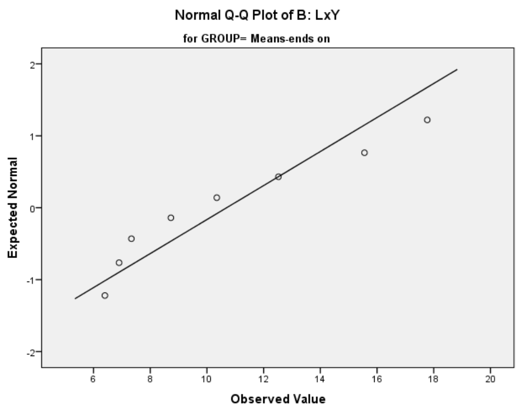

(d) B:LxY group II.

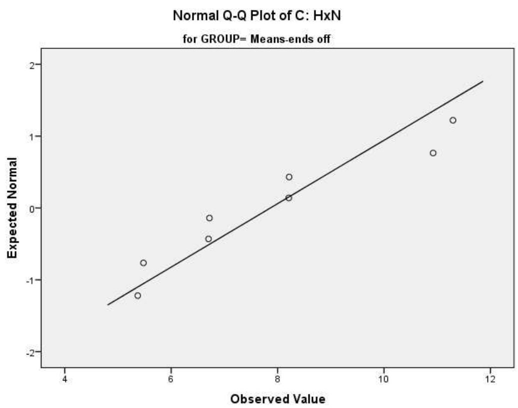

(e) C:HxN group I.

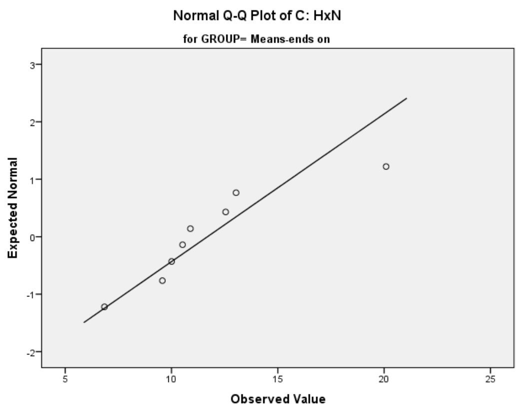

(f) C:HxN group II.

Figure G-4: Advisory response time Q-Q normality plot.

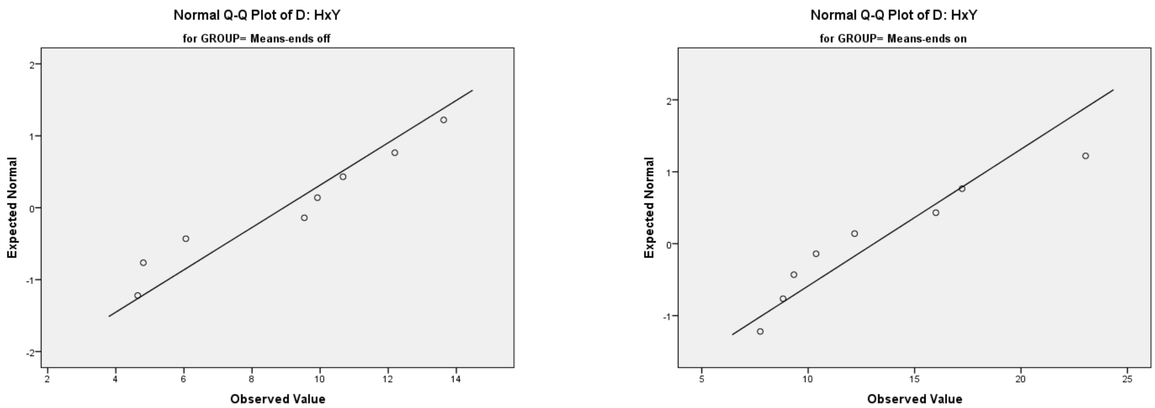

(g) D:HxY group I.

(h) D:HxY group II.

Figure G-4: (Cont.) Advisory response time Q-Q normality plot.

Bibliography

Ali, B., Majumdar, A., Ochieng, W. Y., & Schuster, W. (2013). ADS-B: The Case for London Terminal Manoeuvring Area (LTMA). In *Tenth usa/europe air traffic management research and development seminar* (p. 10).

Borst, C., Mulder, M., & Van Paassen, M. M. (2010, September). Design and Simulator Evaluation of an Ecological Synthetic Vision Display. *Journal of Guidance, Control, and Dynamics*, *33*(5), 1577–1591. Retrieved from http://arc.aiaa.org/doi/abs/10.2514/1.47832 doi: 10.2514/1.47832

Borst, C., Westin, C., & Hilburn, B. (2012). An Investigation into the Use of Novel Conflict Detection and Resolution Automation in Air Traffic Management. *SESAR Innovation Days*(November).

Burns, C. M. (2000, January). Putting it all Together: Improving Display Integration in Ecological Displays. *Human factors*, *42*(2), 226–41. Retrieved from http://www.ncbi.nlm.nih.gov/pubmed/11022882

Cedrini, V., Zacchei, M., Zampognaro, V., Ente, E., Assistenza, N., Spa, V., & Agri, V. (2010). ADS-B 1090ES Implementation : the CRISTAL-MED Project. , *3*, 1–5.

Frank, P. M. (1990). Fault Diagnosis in Dynamic Systems Using Analytical and Knowledge-Based Redundancy: A Survey and Some New Results. *Automatica*, *26*(3), 459–474. Retrieved from http://www.sciencedirect.com/science/article/pii/000510989090018D

Ham, D. H., & Yoon, W. C. (2001). Design of Information Content and Layout for Process Control Based on GoalMeans Domain Analysis. *Cognition, Technology & Work*, 205–223. Retrieved from http://link.springer.com/article/10.1007/s10111-001-8003-z

ICAO. (2005). *Annex 2 to the Convention on International Civil Aviation: Rules of the Air* (Tech. Rep. No. July). Author. Retrieved from http://link.springer.com/chapter/10.1007/978-3-642-25835-0_3

ICAO. (2013). *The Ninth Meeting of the Southeast Asia and Bay of Bengal Sub-regional ADS-B Implementation Working Group (SEA/BOB ADS-B WG/9)* (Tech. Rep.). Beijing.

Isermann, R. (1997). Supervision, Fault-Detection and Fault-Diagnosis Nethodsan Introduction. *Control engineering practice*, *5*(5), 639–652. Retrieved from http://www.sciencedirect.com/science/article/pii/S0967066197000464

Jamieson, G. (2003, October). Bridging the Gap Between Cognitive Work Analysis and Ecological Interface Design. *Proceedings of the Human Factors and Ergonomics Society Annual Meeting*, *47*(3), 273–277. Retrieved from http://pro.sagepub.com/lookup/doi/10.1177/154193120304700305 doi: 10.1177/154193120304700305

Oxford University. (2014). *Oxford Dictionaries Online.* Retrieved 2014, August, from http://www.oxforddictionaries.com/definition/english/interface

Reising, D. V. C., & Sanderson, P. M. (2004, January). Minimal Instrumentation May Compromise Failure Diagnosis with an Ecological Interface. *Human Factors: The Journal of the Human Factors and Ergonomics Society*, *46*(2), 316–33. Retrieved from http://www.ncbi.nlm.nih.gov/pubmed/15359680

Rekkas, C., & Rees, M. (2008). Towards ADS-B Implementation in Europe. *Tyrrhenian International Workshop on Digital Communications - Enhanced Surveillance of Aircraft and Vehicles*, 1–4. Retrieved from http://ieeexplore.ieee.org/lpdocs/epic03/wrapper.htm?arnumber=4649019

St-Cyr, O. (2006a, October). Impact of Sensor Noise Magnitude on Emergent Features of Ecological Interface Design. *Proceedings of the Human Factors and Ergonomics Society Annual Meeting*, *50*(3), 319–323. Retrieved from http://pro.sagepub.com/lookup/doi/10.1177/154193120605000323 doi: 10.1177/154193120605000323

St-Cyr, O. (2006b). *Sensor Noise and Ecological Interface Design: Effects of Noise Magnitude on Operators' Performance and Control Strategies* (Doctoral dissertation). Retrieved from https://tspace.library.utoronto.ca/handle/1807/29504

St-Cyr, O., Jamieson, G. A., & Vicente, K. J. (2013, November). Ecological Interface Design and Sensor Noise. *International Journal of Human-Computer Studies*, *71*(11), 1056–1068. Retrieved from http://linkinghub.elsevier.com/retrieve/pii/S1071581913001031 doi: 10.1016/j.ijhcs.2013.08.005

Torel, Y. (2014). *Is ADS-B Capable of Replacing Radar as a Primary Means of Aircraft Surveillance in the Near Future?* (Tech. Rep.). Delft University of Technology.

Van Dam, S. B. J., Mulder, M., & Van Paassen, M. M. (2008). Ecological Interface Design of a Tactical Airborne Separation Assistance Tool. *IEEE Transactions on Systems, Man and Cybernetics*, *38*(6), 1221–1233.

Velasco, G. A. M. (2010). Analysis of Air Traffic Controller Workload Reduction Based on the Solution Space for the Merging Task. *AIAA Guidance, Naviagtion and Control Conference*(August). Retrieved from http://arc.aiaa.org/doi/pdf/10.2514/6.2010-7541

Vicente, K. J. (1999). *Cognitive Work Analysis; Toward Safe, Productive, and Healthy Computer-Based Work.* Mahwah, New Jersey: Lawrence Erlbaum Associates.

Vicente, K. J. (2002, January). Ecological Interface Design: Progress and Challenges. *Human Factors: The Journal of the Human Factors and Ergonomics Society*, *44*(1), 62–78. Retrieved from http://www.ncbi.nlm.nih.gov/pubmed/12118874

Vicente, K. J., Moray, N., Lee, J. D., Rasmussen, J., Jones, B. G., Brock, R., & Djemil, T. (1996, September). Evaluation of a Rankine Cycle Display for Nuclear Power Plant Monitoring and Diagnosis. *Human Factors: The Journal of the Human Factors and Ergonomics Society*, *38*(3), 506–521. Retrieved from

http://openurl.ingenta.com/content/xref?genre=article&issn=0018-7208&volume=38&issue=
doi: 10.1518/001872096778702033

Vicente, K. J., & Rasmussen, J. (1992). Ecological Interface Design: Theoretical Foundations. *IEEE Transactions on Systems, Man and Cybernetics*, *22*(4). Retrieved from http://ieeexplore.ieee.org/xpls/abs_all.jsp?arnumber=156574

Zhang, J., Liu, W., & Zhu, Y. (2011). Study of ADS-B Data Evaluation. *Chinese Journal of Aeronatics*, *24(4)*, 461–466.